



Search for single production of a heavy vector-like T quark decaying to a Higgs boson and a top quark with a lepton and jets in the final state

The CMS Collaboration*

Abstract

A search for single production of vector-like top quark partners (T) decaying into a Higgs boson and a top quark is performed using data from pp collisions at a centre-of-mass energy of 13 TeV collected by the CMS experiment at the CERN LHC, corresponding to an integrated luminosity of 2.3 fb^{-1} . The top quark decay includes an electron or a muon while the Higgs boson decays into a pair of b quarks. No significant excess over standard model backgrounds is observed. Exclusion limits on the product of the production cross section and the branching fraction are derived in the T quark mass range 700 to 1800 GeV. For a mass of 1000 GeV, values of the product of the production cross section and the branching fraction greater than 0.8 and 0.7 pb are excluded at 95% confidence level, assuming left- and right-handed coupling of the T quark to standard model particles, respectively. This is the first analysis setting exclusion limits on the cross section of singly produced vector-like T quarks at a centre-of-mass energy of 13 TeV.

Published in Physics Letters B as doi:10.1016/j.physletb.2017.05.019.

1 Introduction

Over the past decades several theoretical models have been formulated trying to give new insights into electroweak symmetry breaking and the mechanisms that stabilise the mass of the Higgs boson. Many of these models predict the existence of heavy vector-like quarks. Examples are little Higgs models [1–3], models with extra dimensions [4, 5], and composite Higgs boson models [6–10].

The distinctive property of vector-like quarks is that their left- and right-handed components transform in the same way under the electroweak symmetry group $SU(2)_L \times U(1)_Y$ of the standard model (SM). As a consequence, vector-like quarks can obtain mass through direct mass terms in the Lagrangian of the form $m\bar{\psi}\psi$, unlike the SM chiral quarks, which obtain mass through Yukawa coupling.

The discovery of a Higgs boson by the ATLAS [11] and CMS [12, 13] Collaborations and the electroweak fits within the framework of the SM [14] strongly disfavour the existence of a fourth generation of chiral fermions. Given the limited impact that vector-like quarks have on the properties of the SM Higgs boson, they are not similarly constrained [15].

This letter presents the results of the first search for singly produced vector-like top quark partners with charge $+2/3$ (T) at a centre-of-mass energy of $\sqrt{s} = 13$ TeV. Single production is of particular interest, since its rate dominates over the rate of pair production at large quark masses. Many of the models mentioned above predict that the T quark will predominantly decay to third-generation SM quarks via three channels: tH , tZ , and bW [15]. Searches for T quarks have been performed by the ATLAS and CMS Collaborations setting lower limits on the T quark mass ranging from 715 to 950 GeV for various T quark branching fractions [16–22].

While most of the past searches considered pair production of the T quarks via the strong interaction, the single production mode where the T quark is produced via the weak interaction has recently been investigated by the ATLAS Collaboration [16, 19, 20] at 8 TeV, and is targeted in this letter. The strength of the T quark coupling to electroweak bosons has an effect both on the cross section and the width of the T quark [23]. There are no a priori constraints on the electroweak T quark coupling. Therefore, not only the general coupling to the electroweak sector but the couplings of the T quark to bW , tZ , and tH can also take arbitrary values. The present analysis targets decays of the T quark into a Higgs boson and a top quark. It will be sensitive to the existence of a T quark only if sufficiently large couplings to bW or tZ are present as well, since the T quark production through a Higgs boson is strongly suppressed. An example of a Feynman diagram for this process is shown in Fig. 1.

The analysis is performed on the proton-proton collision data collected during 2015 by the CMS experiment at the CERN LHC at $\sqrt{s} = 13$ TeV. The search is optimised for decays of the T quark into a Higgs boson and a top quark, where the top quark decay includes a lepton (electron or muon) and the Higgs boson is required to decay into b quarks. For a T quark mass in the TeV range, the Higgs boson and the top quark obtain large Lorentz boosts leading to merged jets and nonisolated leptons in the final state. Jet substructure analysis in combination with algorithms for the identification of b quark jets (b tagging) can efficiently identify boosted decays of the Higgs boson into b quark pairs [22]. An additional distinctive feature of the signal is the presence of a jet in the regions close to the beam pipe, a so-called forward jet. This jet results from the light-flavour quark that is produced in association with the T quark. Background processes due to top quark pair production are dominant, followed by W +jets and quantum chromodynamics (QCD) multijet processes.

For every event, a T quark candidate four-momentum is reconstructed, with mass M_T . Events

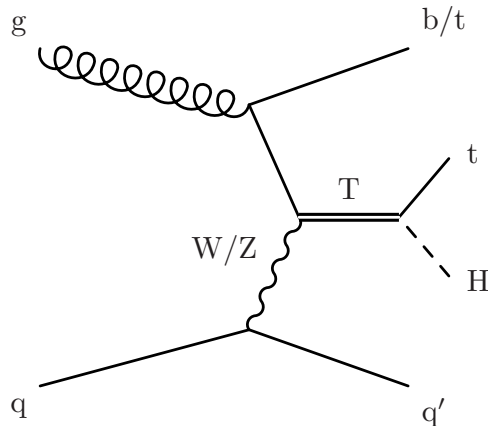


Figure 1: Feynman diagram of the production and decay mechanisms of a vector-like T quark, as targeted in this analysis.

are selected by imposing requirements on the T quark candidate and other attributes of the event. The M_T variable is used as the final discriminant in a combined signal plus background fit to the data. The shape of the total background is estimated from a signal-depleted region in the recorded data.

2 The CMS detector

The central feature of the CMS apparatus is a superconducting solenoid of 6 m internal diameter, providing a magnetic field of 3.8 T. Within the solenoid volume are a silicon pixel and strip tracker, a lead tungstate crystal electromagnetic calorimeter (ECAL), and a brass and scintillator hadron calorimeter (HCAL), each composed of a barrel and two endcap sections. Forward calorimeters extend the coverage provided by the barrel and endcap detectors to regions close to the beam pipe. Muons are measured in gas-ionisation detectors embedded in the steel flux-return yoke outside the solenoid. A more detailed description of the CMS detector, together with a definition of the coordinate system used and the relevant kinematic variables, can be found in Ref. [24].

A particle-flow (PF) algorithm [25, 26] is used to combine information from all CMS subdetectors in order to reconstruct and identify individual particles in the event: photons, electrons, muons, and charged and neutral hadrons. The energy of photons is directly obtained from the ECAL measurement. The energy of electrons is determined from a combination of the electron momentum at the primary interaction vertex determined by the tracker, the energy of the corresponding ECAL cluster, and the energy sum of all bremsstrahlung photons spatially compatible with originating from the electron track. The momentum resolution for electrons with transverse momentum $p_T \approx 45$ GeV and above from $Z \rightarrow ee$ decays ranges from 1.7% for non-showering electrons in the barrel region to 4.5% for showering electrons in the endcaps [27]. Muons are measured in the pseudorapidity range $|\eta| < 2.4$ with detection planes made using three technologies: drift tubes, cathode strip chambers, and resistive-plate chambers. Matching muons to tracks measured in the silicon tracker results in a relative p_T resolution of 1.2–2.0% for muons with $20 < p_T < 100$ GeV in the barrel and better than 6% in the endcaps. The p_T resolution in the barrel is better than 10% for muons with p_T up to 1 TeV [28]. The energy of charged hadrons is determined from a combination of their momentum measured in the tracker and the matching of ECAL and HCAL energy deposits, corrected for the response function of the calorimeters to hadronic showers. Finally, the energy of neutral hadrons is obtained from the corresponding corrected ECAL and HCAL energy.

Jets are reconstructed from the individual particles identified by the PF event algorithm, clustered by the anti- k_t algorithm [29, 30]. Two different jet sizes are used independently: jets with a size parameter of 0.4 (“AK4 jets”) and 0.8 (“AK8 jets”). Jet momentum is determined as the vector sum of the charged particle momenta in the jet that are identified as originating from the primary interaction vertex, and the neutral particle momenta. An area-based correction is applied to jet energies to take into account the contribution from additional proton-proton interactions within the same or adjacent bunch crossings (“pileup”) [31]. The energy of a jet is found from simulation to be within 5–10% of the true jet momentum at particle level over the entire p_T spectrum and detector acceptance. Jet energy corrections are derived from simulation, and are confirmed with in situ measurements of the energy balance in dijet and photon+jet events [32]. A smearing of the jet energy is applied to simulated events to mimic detector resolution effects observed in data. For the identification of b jets, the combined secondary vertex b tagging algorithm is used [33]. The algorithm uses information from secondary b hadron decay vertices to distinguish b jets from other jet flavours. The jet energy resolution is typically 15% at 10 GeV, 8% at 100 GeV, and 4% at 1 TeV. Jets are reconstructed up to $|\eta| = 5$ while b tagging is restricted by the tracker acceptance to $|\eta| < 2.4$.

The missing transverse momentum vector \vec{p}_T^{miss} is defined as the negative vector sum of the p_T of all PF particle candidates in an event. Its magnitude is referred to as E_T^{miss} .

3 Data and simulated samples

Events in the electron channel are selected using an electron trigger, which requires an electron with $p_T > 45$ GeV and the additional presence of at least two jets, with $p_T > 200$ GeV and 50 GeV, respectively for the jets with the highest and second highest p_T . Events in the muon channel are collected with a single-muon trigger, requiring the presence of a muon candidate with $p_T > 45$ GeV and $|\eta| < 2.1$. The muon trigger does not require a jet. Neither of the triggers places any requirement on the isolation of the leptons. If an event is selected by both the electron and the muon trigger, which happens almost exclusively in top quark pair events containing an electron and a muon, it is assigned to the muon channel. The data collected with the muon trigger correspond to a luminosity of $\mathcal{L} = 2.3 \text{ fb}^{-1}$, while the electron trigger provides a luminosity $\mathcal{L} = 2.2 \text{ fb}^{-1}$.

Signal samples are generated using MADGRAPH 5_aMC@NLO 2.2.2 [34] at leading order (LO) QCD accuracy. The cross section to produce a heavy T quark decaying to top quark and Higgs boson in association with a bottom or top quark is set to 1 pb unless indicated differently. Signal masses are simulated between 700 and 1800 GeV in steps of 100 GeV, assuming a fixed T quark width of 10 GeV. This width corresponds to a narrow width approximation, meaning that the experimental resolution is much larger than the width used in generating the samples. Generation of both the T quark and its antiquark are included, with the positive charge having a higher occurrence because of the larger density of positively charged u quarks in the proton. Only the left- (right-) handed T quark chiralities in association with a bottom (top) quark are considered, as only those are allowed in the singlet (doublet) scenario of the simplest Simplified Model [23]. Left- and right-handed production of the T quark are simulated in separate samples.

Background events from top quark pair production and electroweak production of a single top quark in the tW-channel are simulated at next-to-leading order (NLO) with the POWHEG 2.0 generator [35–38]. The MADGRAPH 5_aMC@NLO at NLO accuracy is used to generate samples of single top quarks in the s- and t-channels. The generation of the W+jets and Z+jets events is performed at LO with the MADGRAPH 5_aMC@NLO, with up to four partons included in the

matrix element calculations, matched to parton showers using the so-called MLM scheme [39]. All samples are interfaced with PYTHIA 8.212 [40, 41], tune CUETP8M1 [42] for the description of hadronisation and fragmentation. The QCD multijet background events are generated with PYTHIA for both matrix element and showering descriptions.

All samples are generated using NNPDF 3.0 [43] parton distribution functions (PDFs) either at LO or at NLO, to match the precision of the matrix element calculation. The effects of pileup are simulated in all samples by adding simulated minimum bias events to the hard scattering process, according to a distribution having an average multiplicity of 11 collisions per bunch crossing, as observed in data.

All events are processed through a full simulation of the CMS detector using GEANT4 [44, 45].

4 Event reconstruction and selection

Primary vertices are reconstructed using a deterministic annealing filtering algorithm [46]. The leading vertex of the event is defined as the one with the largest sum of squared p_T of associated tracks. Its position is reconstructed using an adaptive vertex fit [47] and is required to be within 24 cm in the z direction and 2 cm in the x - y plane of the nominal interaction point.

Events are required to have at least one lepton. For large T quark masses, the top quark from the $T \rightarrow tH$ decay has a significant Lorentz boost causing its products to be approximately collinear. Thus as the lepton is not isolated from the b quark jet (“ b jet”), no conventional isolation requirement (i.e. requiring the energy deposited in a cone around the lepton to be small) is applied. In order to suppress QCD multijet events with a lepton (electron or muon) contained within an AK4 jet, the selection criteria $\Delta R(\ell, j) > 0.4$ or $p_T^{\text{rel}}(\ell, j) > 40 \text{ GeV}$ are applied, where ℓ indicates the lepton and j indicates the AK4 jet with lowest angular separation from the lepton. The angular distance is defined as $\Delta R = \sqrt{(\Delta\eta)^2 + (\Delta\phi)^2}$, where $\Delta\phi$ ($\Delta\eta$) is the difference in azimuthal angle (pseudorapidity) between the AK4 jet and the lepton, and p_T^{rel} is the projection of the three-momentum of the lepton onto a plane perpendicular to the jet axis. In addition to this selection, electrons (muons) must have $p_T > 50$ (47) GeV and $|\eta| < 2.5$ (2.1), to fall within a region where the trigger efficiency is constant. In the case of more than one reconstructed lepton in the given channel, only the lepton with the highest p_T is used in the evaluation of physics quantities needed for this analysis and shown in the plots below. The lepton isolation and trigger selection efficiencies are measured in the data and simulation as a function of η and p_T of the lepton and are found to agree within their uncertainties.

All AK4 jets are required to have $p_T > 30 \text{ GeV}$. If a selected lepton is found within a cone of $\Delta R(j, \ell) < 0.4$ around the jet axis, the lepton four-momentum is subtracted from the uncorrected jet four-momentum and all jet energy corrections are applied thereafter. AK4 jets with $|\eta| > 2.4$ are defined as “forward jets”. An event must have at least two AK4 jets. The leading (subleading) AK4 jet p_T is required to exceed 250 (70) GeV in the electron channel and 100 (50) GeV in the muon channel. The different p_T thresholds for the two channels are due to the tighter criteria of the electron trigger, which selects events with two high- p_T jets (Section 3).

Since the decay of a heavy T quark would produce high-energy final-state particles, all events are required to have $S_T > 400 \text{ GeV}$, where S_T is defined as the scalar sum over E_T^{miss} , the p_T of the lepton and the transverse momenta of all selected AK4 jets in the event.

The AK8 jets are required to have $p_T > 200 \text{ GeV}$ and $|\eta| < 2.4$. The modified mass drop tagger algorithm [48], also known as the “soft-drop” algorithm with angular exponent $\beta = 0$, soft threshold $z_{\text{cut}} < 0.1$, and characteristic radius $R_0 = 0.8$ [49], is used to remove soft, wide-

angle radiation from the jet. Subjets of AK8 jets are identified in the last reclustering step of the soft-drop algorithm. The soft-drop jet mass scale and resolution have been estimated using a $t\bar{t}$ control region. This control region is defined by the baseline selection (see below) and additionally requiring two b-tagged AK4 jets as well as the N-subjettiness ratio τ_2/τ_1 to be smaller than 0.4 [50, 51] for the Higgs boson candidate (see below). The mass scale is found to be compatible between data and simulation within uncertainties. A degradation of the jet mass resolution of 10% is applied in the simulation to match the resolution found in the data.

For the identification of b jets, the combined secondary vertex b tagging algorithm is used. In this analysis, it is only applied to the final two soft-drop subjets of AK8 jets. A working point that typically yields b tagging efficiencies of approximately 80% and misidentification rates from light-flavour jets of about 10% in $t\bar{t}$ events [33] is chosen. The b tagging of subjets results in a better performance compared to the b tagging of AK4 jets in $t\bar{t}$ events, reducing the misidentification rate at the working point by a factor of approximately two.

In order to identify decays of the boosted Higgs boson to b quark pairs (H tagging) [22], the soft-drop mass of the jet, M_H , is required to be within $90 < M_H < 160$ GeV. At least one Higgs boson candidate is required to be present and to have an angular separation of $\Delta R(H, \ell) > 1.0$ from the lepton. The number of b tagged subjets of the Higgs boson candidate is used to define the signal and background control regions.

To reconstruct the top quark, its decay into a bottom quark and a W boson, with the W boson subsequently decaying into a muon or electron and a neutrino, is assumed. Using the x and y components of \vec{p}_T^{miss} , the lepton four-momentum, and the nominal mass of the W boson (80.4 GeV), [52] the z component of the neutrino momentum is reconstructed by solving a quadratic equation, resulting in up to two solutions. If a complex solution is obtained, only the real part is used. Combining the four-momenta of these neutrino hypotheses and the lepton, up to two W boson candidates are obtained. Each W boson candidate is paired to every central AK4 jet in the event, giving a number of reconstruction hypotheses for the top quark. In order to accommodate final-state radiation from the top quark, further top quark reconstruction hypotheses are found by the addition of one more AK4 jet, such that one top quark candidate is established for every single AK4 jet and every possible combination of two AK4 jets. The b tagging information is not used in the top quark reconstruction.

Top quark and Higgs boson candidates are combined into pairs. Combinations are rejected if any AK4 jet (j_i) of the top quark candidate overlaps with the Higgs boson candidate within $\Delta R(j_i, H) < 1.0$. This requirement ensures that there is no overlap or double counting of jets from the two jet collections with jet sizes 0.4 and 0.8. The pair of candidates yielding the smallest χ^2 value is used in the following analysis, where the χ^2 function is defined as follows:

$$\chi^2 = \left(\frac{M_{H,MC} - M_H}{\sigma_{M_H,MC}} \right)^2 + \left(\frac{M_{t,MC} - M_t}{\sigma_{M_t,MC}} \right)^2 + \left(\frac{\Delta R(t, H)_{MC} - \Delta R(t, H)}{\sigma_{\Delta R,MC}} \right)^2.$$

Here, M denotes the mass of a candidate, and the H and t subscripts stand for the Higgs boson and top quark candidates, respectively. The ‘‘MC’’ subscript denotes that a quantity is derived from the signal simulation, using the correct pairing of the reconstructed objects based on Monte Carlo information. Other quantities are obtained from the pair of top quark and Higgs boson candidates.

After event reconstruction, the selection is further refined by requiring a large separation of $\Delta R(t, H) > 2.0$ between the top quark and Higgs boson candidates. The top quark candidate must have $p_T > 100$ GeV.

The selection criteria described above define the “baseline selection”. Distributions of some relevant variables after the baseline selection are shown in Figs. 2 and 3. The background contributions are estimated from simulated events. The hypothetical signal is scaled to a cross section of 20 pb as indicated in the legend of the figure. The simulated background events and data are found to be in agreement.

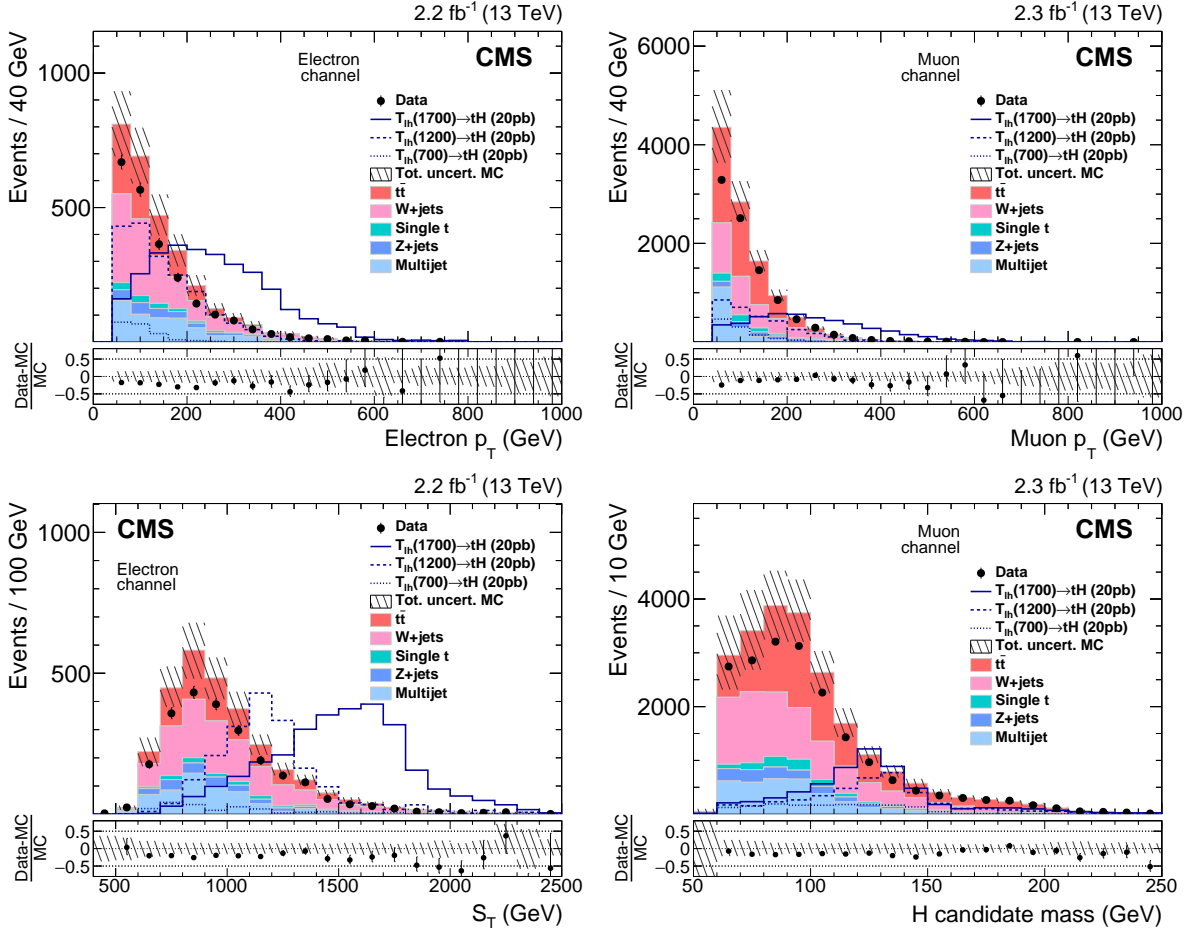


Figure 2: Distributions of kinematic variables after baseline selection. Electron and muon p_T distributions are depicted in the upper-left and upper-right panels. The lower-left panel shows S_T in the electron channel while the soft-drop mass of the Higgs boson candidate in the muon channel is depicted in the lower right. The different background contributions are shown using full histograms while the open histograms are signal yields and the data are shown as solid circles. The hatched bands represent the statistical and systematic uncertainties of the simulated event samples. The systematic uncertainties include those discussed in Section 6, except the forward jet uncertainty. Signal cross sections are enhanced to 20 pb.

After the baseline selection, two event categories are defined. The signal region is used for signal extraction and is defined by requiring that both soft-drop subjects of the Higgs boson candidate are b tagged and that there is at least one forward jet. The “control region” for background estimation is defined by requiring the absence of forward jets and that exactly one of the soft-drop subjects of the Higgs boson candidates is b tagged. In addition, two validation regions with zero subjet b-tags, “region A” and “region B”, are defined. These validation regions are used to cross-check the background estimation method as described in Section 5. The event selection criteria of all regions are summarised in Table 1.

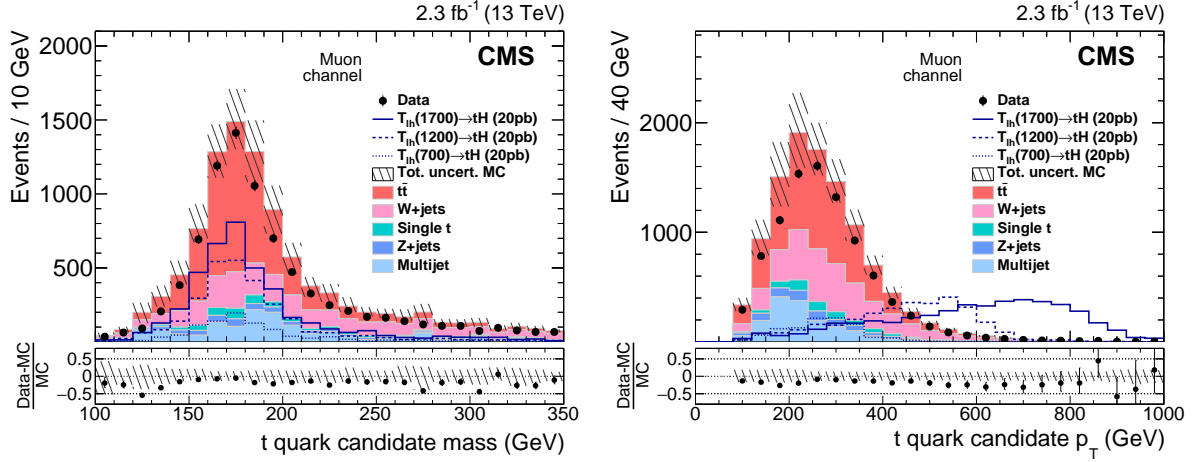


Figure 3: Mass (left) and p_T (right) distributions of the reconstructed top quark candidate in the muon channel after the baseline selection. The different background contributions are shown using full histograms while the open histograms are signal yields and the data are shown as solid circles. The hatched bands represent the statistical and systematic uncertainties of the simulated event samples. The systematic uncertainties include those discussed in Section 6, except the forward jet uncertainty. Signal cross sections are enhanced to 20 pb.

Table 1: Event selection criteria: required number of b tagged subjects for the Higgs boson candidate, and number of forward jets.

Region	Signal region	Control region	Validation region A	Validation region B
Subjet b tags (H candidate)	exactly 2	exactly 1	exactly 0	exactly 0
Forward jets	at least 1	exactly 0	exactly 0	at least 1

The T quark candidate is reconstructed from the sum of the Higgs boson and the top quark candidate four-momenta. The M_T is used as the discriminating variable in the limit setting procedure. Figure 4 shows the simulated signal and background distributions of M_T in the signal region. In the electron (muon) channel 35 (134) data events are selected, as summarised in Table 2 along with the event yields and selection efficiencies for three of the signal samples. The signal selection efficiency is depicted as a function of the generated T quark mass in Fig. 5. The denominator of the efficiency includes all decay modes of the top quark and the Higgs boson, i.e. the product of the branching fractions for the top quark decaying to final states including a lepton, and the Higgs boson decaying to bottom quarks, amounting to approximately 8%, is included in the signal selection efficiency. The selection efficiency is notably larger for the right-handed signal samples, because of the harder p_T spectrum of leptons stemming from right-handed T quarks, and the presence of additional leptons from the associated top quark production.

5 Background Estimate

The combined shape of the M_T distribution of all background processes is provided by the data in the control region. It is used together with the simulated signal distribution in a fit of signal plus background distributions to the observed data. The normalization of the background distribution is estimated in the fit.

Figure 6 shows the reconstructed mass of the T quark candidates in the control region, where

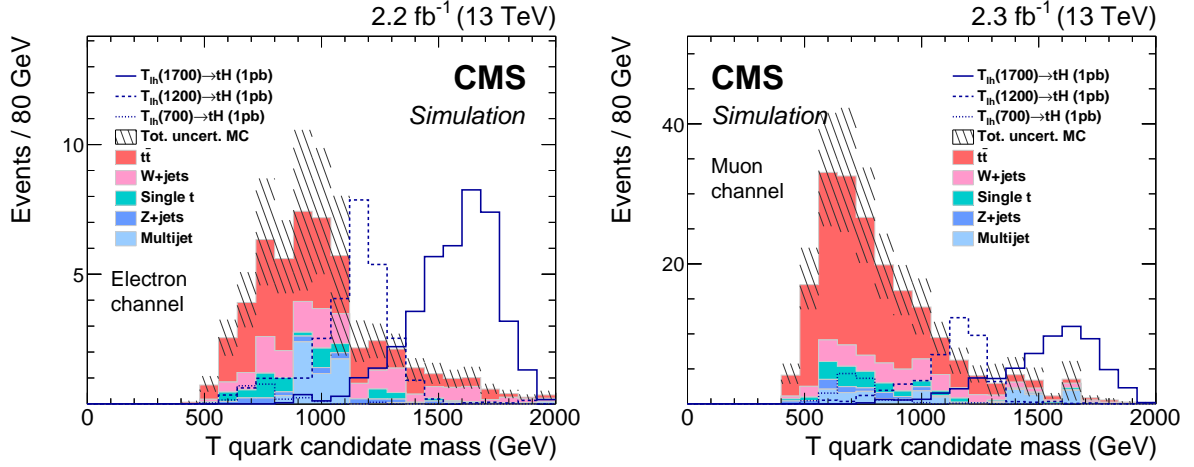


Figure 4: Vector-like T quark candidate mass in the signal region for the electron (left) and muon (right) channels. The different background contributions are shown using full histograms while the open histograms are signal yields and the data are shown as solid circles. The hatched bands represent the statistical and systematic uncertainties of the simulated event samples. The systematic uncertainties include those discussed in Section 6.

Table 2: Number of selected events N_{sel} and selection efficiency ϵ_{sel} for the signal region including both statistical (stat) and systematic (sys) uncertainties. For the background, the post-fit value (as described in Sections 5 and 7) is quoted. The left- (right-) handed T quark production in association with a bottom (top) quark is denoted by a subscript lh (rh) and following b (t). All signal samples are normalized to a cross section of 1 pb, i.e. the product of the branching fractions for the top quark decaying to final states including a lepton, and the Higgs boson decaying to bottom quarks, amounting to approximately 8%, is included in the signal selection efficiency.

	Electron channel		Muon channel	
	$N_{\text{sel}} \pm \text{stat} \pm \text{sys}$	$\epsilon_{\text{sel}} (\%)$	$N_{\text{sel}} \pm \text{stat} \pm \text{sys}$	$\epsilon_{\text{sel}} (\%)$
$T_{\text{lh}}(700) \text{ b}$	$1.2 \pm 1.1 \pm 0.3$	0.05	$6.0 \pm 2.4 \pm 1.2$	0.26
$T_{\text{lh}}(1200) \text{ b}$	$14.4 \pm 0.9 \pm 2.6$	0.65	$22.8 \pm 1.1 \pm 3.9$	0.98
$T_{\text{lh}}(1700) \text{ b}$	$15.3 \pm 0.9 \pm 2.7$	0.69	$22.9 \pm 1.1 \pm 3.9$	0.99
$T_{\text{rh}}(700) \text{ t}$	$6.4 \pm 2.5 \pm 1.1$	0.29	$14.2 \pm 3.8 \pm 2.3$	0.61
$T_{\text{rh}}(1200) \text{ t}$	$20.3 \pm 1.0 \pm 3.4$	0.91	$33.6 \pm 1.3 \pm 5.4$	1.45
$T_{\text{rh}}(1700) \text{ t}$	$21.7 \pm 1.1 \pm 3.5$	0.98	$34.6 \pm 1.4 \pm 5.7$	1.49
	$N_{\text{sel}} \pm \text{stat} \pm \text{fit}$		$N_{\text{sel}} \pm \text{stat} \pm \text{fit}$	
Background (post-fit)	$34.8 \pm 1.4 \pm 4.2$		$133 \pm 3 \pm 16$	
Data	35		134	

the signal cross section is increased by a factor of 20. Data and simulation is observed to agree. The control region features a signal-to-background ratio of approximately 5% of that found in the signal region and can therefore be used to estimate the background with low signal contamination.

Both the signal and control regions contain 50–60% top quark pair background and 20–30% W+jets background. The relative background composition is therefore similar in the signal and control regions. Also the kinematic configuration of the top quark and Higgs boson candidates are similar. These two features facilitate the derivation of the background shape from the control region in data without any further corrections. This procedure is validated by a shape

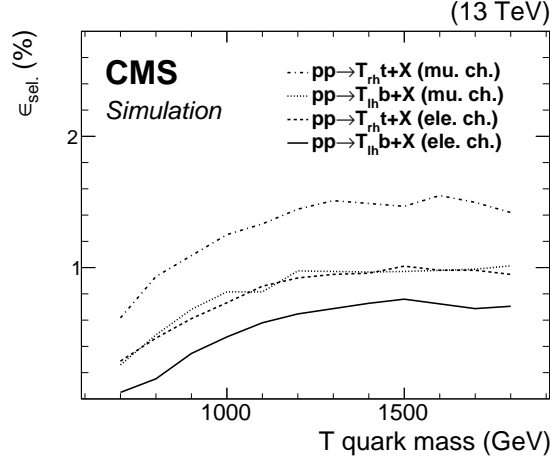


Figure 5: Selection efficiency ϵ_{sel} for the signal, i.e. the product of the branching fractions for the top quark decaying to final states including a lepton, and the Higgs boson decaying to bottom quarks, amounting to approximately 8%, is included in the signal selection efficiency. Left-handed (denoted by lh) and right-handed (denoted by rh) couplings of the T quark to SM particles in associated production with bottom and top quarks, respectively, are shown separately.

comparison of the M_T distribution between the signal and control regions in simulated events, as shown in Fig. 7. The compatibility of the distributions is evaluated with a χ^2 test [53], including the statistical uncertainties of the simulation as weights in the test. The p-values obtained in the electron and muon channels are 0.22 and 0.09, respectively. Therefore, the M_T distributions are assumed to be compatible in the signal and control regions. In addition Fig. 7 shows further cross checks using zero subjet b tags on the Higgs boson candidate, thereby enriching the contribution of the W+jets and QCD backgrounds. Also these regions are in good agreement.

The aforementioned shape comparison is repeated for systematic uncertainties that can change the shape of the M_T distribution in either the signal or the control region. These are the jet energy scale and resolution uncertainties, as well as uncertainties in the b tag status of a Higgs boson candidate subjet. Background cross sections are varied by twice their uncertainty, except for the multijet background, which is varied by half the estimated value. Each variation in a systematic uncertainty is applied consistently in both regions.

The compatibility between the validation regions and the control region is also checked in data, as shown in Fig. 8. Agreement between the corresponding regions is observed in all cases.

In the control region, 632 (2949) events are selected in the electron (muon) channel. These relatively large numbers of events ensure that the statistical uncertainty is negligible compared to that in the signal region. In Fig. 9 the background estimate is shown with the distribution of M_T in data.

6 Systematic Uncertainties

Sources of systematic uncertainty may influence the rate and shape of the signal predictions as well as the shape of the background distribution. The background shape uncertainty is taken as the uncertainty in each bin of the distribution of its estimate. Note that there is no rate uncertainty associated with the background prediction described in Section 5, since its normalization is not used to obtain the final results. In the above figures, several rate and

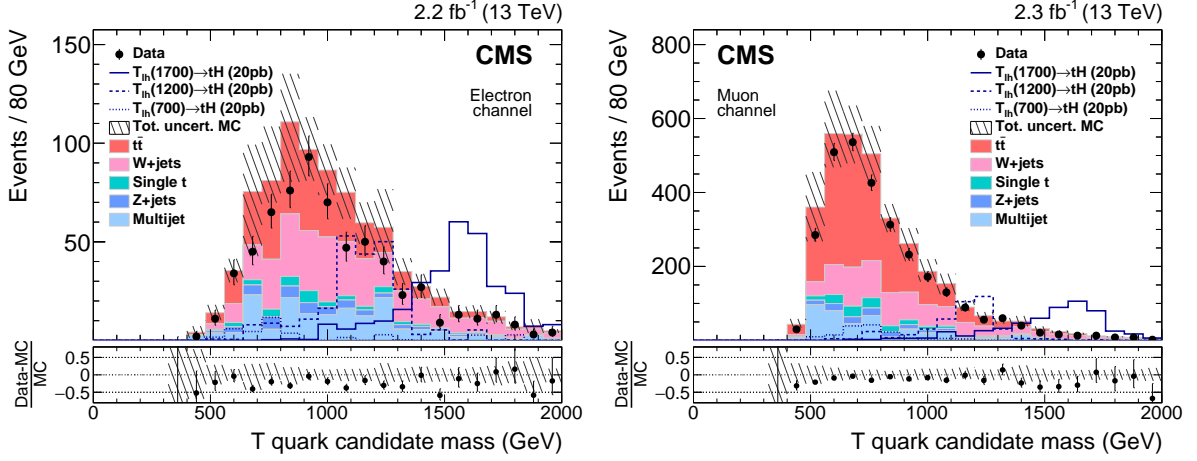


Figure 6: Vector-like T quark candidate mass in the control region for the electron (left) and muon (right) channels. Signal samples are normalized to 20 pb, which is a factor of 20 larger than what is used in Figure 4. The shape of the data distribution provides the background estimate. The different background contributions are shown using full histograms while the open histograms are signal yields and the data are shown as solid circles. The hatched bands represent the statistical and systematic uncertainties of the simulated event samples. The systematic uncertainties include those discussed in Section 6, except the forward jet uncertainty.

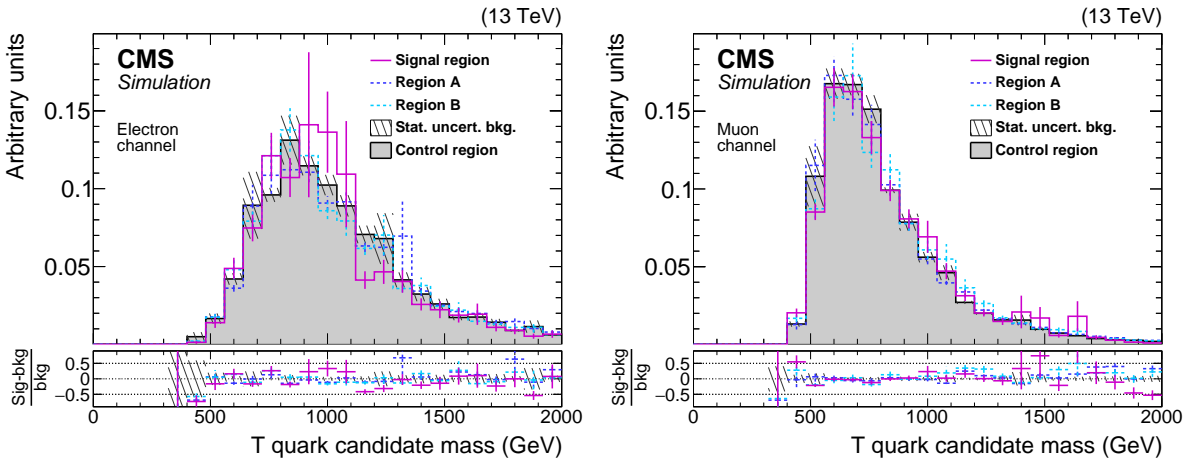


Figure 7: Shape comparison of the T quark candidate mass distributions in the signal (violet solid line) and control (shaded histogram) regions as well as the validation regions A (dark blue dashed line) and B (light blue dashed line) for the electron (left) and muon (right) channels. The distributions show the sum of all simulated backgrounds, with the statistical uncertainties indicated as the error bars (signal region) or the hatched band (control region).

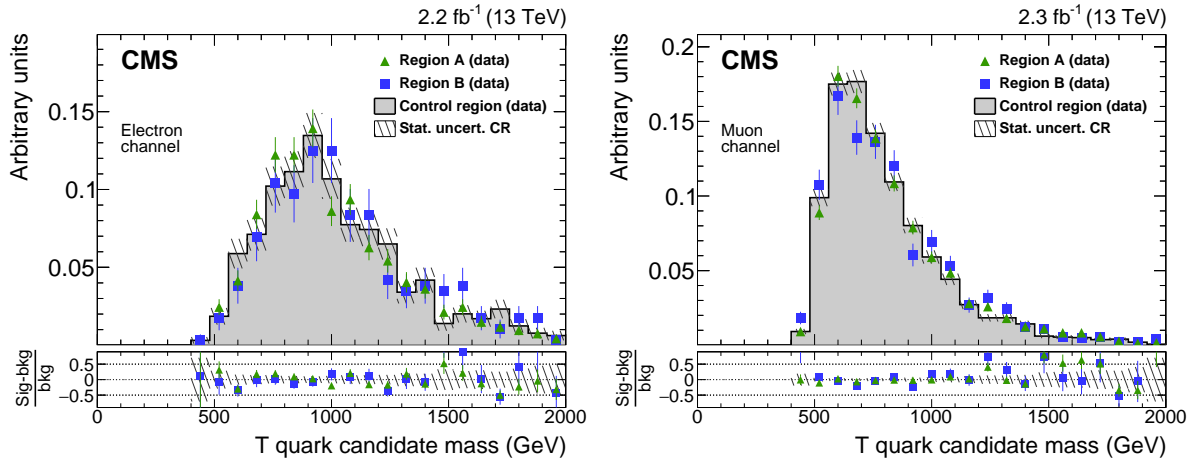


Figure 8: Shape comparison of the T quark candidate mass distributions in the control region (shaded histogram) regions and the validation regions A (green) and B (blue) for the electron (left) and muon (right) channels in data.

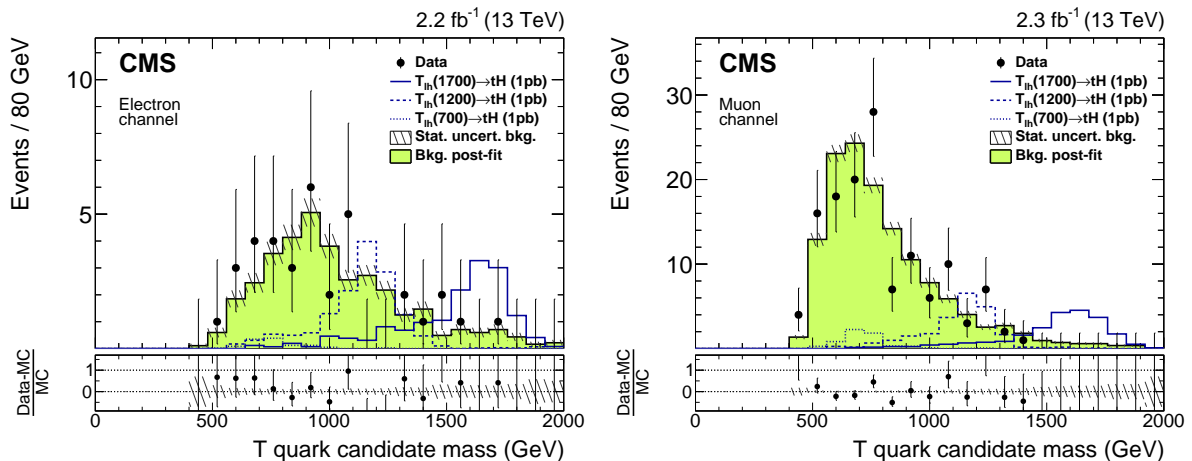


Figure 9: Final background, data, and expected signal distributions in M_T in the signal region for the electron (left) and muon (right) channels. The hatched uncertainty band shows the statistical uncertainty in the background prediction, which is used as the shape uncertainty in the fit, as detailed in Section 6. The normalization of the background estimate is taken from the fit, its uncertainty is 12% (not included in the hatched uncertainty band).

shape uncertainties are considered, for the simulations of both the signal and the background. The one with the largest effect on the final result originates from the uncertainty in the forward jet selection efficiency. The next largest contributions arise from the uncertainties in the b tag efficiency and jet energy corrections. The impacts of the systematic uncertainties on the event rates are listed in Table 3.

Table 3: Impacts of the largest systematic uncertainties in the signal event yields. The signal samples for $T_{lh}b$ production are shown. The uncertainties in the forward jet, and lepton isolation and trigger are rate uncertainties, all other uncertainties are evaluated bin-by-bin. All values are reported as percentage of the signal event yield.

	Electron channel			Muon channel		
	$T_{lh}(700)$	$T_{lh}(1200)$	$T_{lh}(1700)$	$T_{lh}(700)$	$T_{lh}(1200)$	$T_{lh}(1700)$
b tagging, heavy flavour	7.8	7.6	8.7	6.0	7.5	8.5
b tagging, light flavour	0.7	0.7	0.5	1.2	0.6	0.7
Forward jet	15	15	15	15	15	15
Jet energy resolution	7.0	0.6	0.2	0.2	2.3	0.9
Jet energy scale	9.0	4.2	4.9	3.8	3.8	4.4
Lepton isolation and trigger	5.0	5.0	5.0	5.0	5.0	5.0
Soft-drop mass	3.1	1.1	0.3	0.5	0.3	1.3
PDF	4.8	2.7	4.2	4.8	2.8	4.1
Luminosity	2.7	2.7	2.7	2.7	2.7	2.7
Pileup	1.4	0.6	0.1	1.3	0.7	1.1

Scale factors for the b tagging efficiency are applied to simulated events to match the b tagging performance observed in data [33]. The scale factors have a systematic uncertainty of 2–5% for jets originating from b hadrons, 4–10% for c quark jets and 7–10% for light-flavour jets, all depending on the p_T of the jet. Those uncertainties are propagated to the final result, where the uncertainties for heavy-flavour (b and c) jets and light-flavour (u, d, s, g) jets are treated as correlated within their group, but the uncertainties for heavy-flavour jets are assumed to be uncorrelated with those for light-flavour jets.

Jet energy scale and resolution corrections depend on the jet p_T and η . The associated uncertainties are typically a few percent. The resulting uncertainty in the signal yield is derived by applying the $\pm 1\sigma$ variations simultaneously to AK4 and AK8 jets and also propagating the variation of jet momenta into the calculation of E_T^{miss} at the same time. The $\pm 1\sigma$ variations for the resolution smearing in the soft-drop mass are evaluated separately. Additionally, as the reconstruction efficiency of forward jets has been observed to be larger in the simulation compared to the data, a rate uncertainty of $\pm 15\%$ is assigned to the signal samples. This uncertainty is determined by evaluating the event selection efficiency using forward jets in two control regions requiring an event to be selected by the baseline selection and additionally having either zero subjet b tags or exactly one, in association with the H boson candidate. The central region is well modelled by the simulation.

To estimate the uncertainty in the pileup simulation, a variation of $\pm 5\%$ in the inelastic cross section value [54], controlling the average pileup multiplicity, is used. The uncertainty in the luminosity measurement is $\pm 2.7\%$ [55]. Systematic identification and trigger uncertainties for electrons and muons are taken into account for the signal processes. The combined trigger and lepton isolation ($\Delta R(\ell, j)$ or $p_T^{\text{rel}}(\ell, j)$) selection efficiency has a rate uncertainty of $\pm 5\%$. For the PDF uncertainty the complete set of NNPDF 3.0 PDF eigenvectors are evaluated, following the PDF4LHC prescription [56].

7 Results

No significant deviation is observed from the shape predicted by the SM (see Fig. 9). The p -values of the compatibility tests between the predicted and observed distributions are 0.97 and 0.51 in the electron and muon channels, respectively.

Exclusion limits are set on the product of the production cross section and the branching fraction for single production of a vector-like T quark decaying to a top quark and a Higgs boson. The 95% confidence level (CL) exclusion limits are derived with a Bayesian statistical method [57, 58], where background and signal templates in the M_T distribution are used to make a combined fit to the data in the electron and muon channels. Systematic uncertainties are included as nuisance parameters. For rate-only uncertainties a log-normal prior is assigned. A flat prior is used for the signal strength. Shape uncertainties in the signal templates are taken into account using template morphing with cubic-linear interpolation, where the cubic interpolation is used up to the one sigma deviation and the linear interpolation beyond that. For the background normalization a Gaussian prior with 100% width is used. The statistical uncertainty in the background estimate is included with the ‘‘Barlow-Beeston light’’ method [59], which uses a Gaussian approximation of the uncertainty in each bin. A bias-test is performed by injecting a signal into the fitted data. The biases are observed to be negligible.

The obtained exclusion limits are compared with predictions from two benchmark models. For $T_{lh}b$ production, branching fractions of 50/25/25% for the T quark decay to $bW/tZ/tH$ are considered. These branching fractions correspond to the predictions for a vector-like isospin singlet. A scenario with neutral currents only and equal couplings to tZ and tH is used for $T_{rh}t$ production (0/50/50%), corresponding to the prediction for an isospin doublet. Signal cross sections are taken from NLO calculations [23, 60] and multiplied with a factor of 0.25 and 0.5 in order to accommodate the branching fraction $\mathcal{B}(tH) = \mathcal{B}(bW)/2$ and $\mathcal{B}(tH) = \mathcal{B}(tZ)$ for $T_{lh}b$ and $T_{rh}t$ production, respectively. Single vector-like quark production is parametrised with a coupling constant to the electroweak sector. For the coupling of a left- (right-) handed T quark to a quark and boson pair, qV , the coupling strength, as defined in Ref. [23], of $c_{L(R)}^{bW(tZ)} = 0.5$ is assumed in production, where c is a factor multiplying the weak coupling constant g_w . For a coupling parameter of 0.5, it has been verified that the experimental resolution is much larger than the width of the T quark in the simplified model.

In the simplest Simplified Model [23], only the left- (right-) handed couplings are allowed for the singlet (doublet) scenarios, i.e. $c_{R(L)}^{bW(tZ)} = 0$, simultaneously for production and decay of the T quark. Therefore, only fully left- (right-) handed polarisations are considered for the exclusion limits.

Figure 10 shows the 95% CL upper limits on the product of the cross section and the branching fraction, along with the predictions of the simplest Simplified Model with coupling to third generation SM quarks only. It can be seen that the excluded cross sections are an order of magnitude higher than the predictions, and the current data do not place constraints on this particular model. This is the first search for singly produced VLQ by the CMS Collaboration. In the future, results in this channel will become more sensitive by combining results with other final states, and it is anticipated that such Simplified Model cross sections will be probed with the large expected LHC Run 2 dataset.

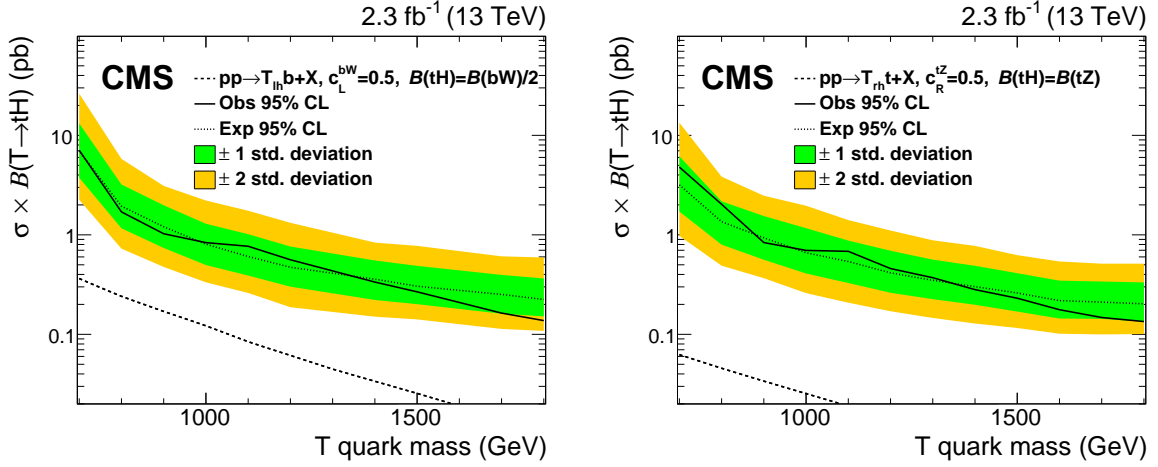


Figure 10: Exclusion limits on the product of the cross section and the branching fraction of single T quark production and $T \rightarrow tH$ decay. A simultaneous fit is made to the electron and muon channels. Left- (right-) handed T quark production in association with a bottom (top) quark is shown in the left- (right-) diagram.

8 Summary

A search for a singly produced vector-like T quark decaying to a top quark and a Higgs boson has been presented, where the top quark decay includes an electron or a muon and the Higgs boson decays into a pair of b quarks. For every event, the four-momentum of the vector-like T quark candidate is reconstructed and its mass is evaluated. No excess over the estimated backgrounds is observed. Upper limits are placed on the product of the cross section and the branching fraction for vector-like T quarks to a top quark and a Higgs boson in the mass range of 700 to 1800 GeV, at 95% confidence level. For a T quark with a mass of 1000 GeV with left- (right-) handed coupling to standard model particles, we exclude a value of the product of the production cross section and the branching fraction greater than 0.8 (0.7) pb. This is the first analysis setting exclusion limits on the cross section of singly produced vector-like T quarks at a centre-of-mass energy of 13 TeV.

Acknowledgments

We congratulate our colleagues in the CERN accelerator departments for the excellent performance of the LHC and thank the technical and administrative staffs at CERN and at other CMS institutes for their contributions to the success of the CMS effort. In addition, we gratefully acknowledge the computing centres and personnel of the Worldwide LHC Computing Grid for delivering so effectively the computing infrastructure essential to our analyses. Finally, we acknowledge the enduring support for the construction and operation of the LHC and the CMS detector provided by the following funding agencies: BMWFW and FWF (Austria); FNRS and FWO (Belgium); CNPq, CAPES, FAPERJ, and FAPESP (Brazil); MES (Bulgaria); CERN; CAS, MoST, and NSFC (China); COLCIENCIAS (Colombia); MSES and CSF (Croatia); RPF (Cyprus); SENESCYT (Ecuador); MoER, ERC IUT, and ERDF (Estonia); Academy of Finland, MEC, and HIP (Finland); CEA and CNRS/IN2P3 (France); BMBF, DFG, and HGF (Germany); GSRT (Greece); OTKA and NIH (Hungary); DAE and DST (India); IPM (Iran); SFI (Ireland); INFN (Italy); MSIP and NRF (Republic of Korea); LAS (Lithuania); MOE and UM (Malaysia); BUAP, CINVESTAV, CONACYT, LNS, SEP, and UASLP-FAI (Mexico); MBIE (New Zealand); PAEC (Pakistan); MSHE and NSC (Poland); FCT (Portugal); JINR (Dubna); MON, RosAtom,

RAS, and RFBR (Russia); MESTD (Serbia); SEIDI and CPAN (Spain); Swiss Funding Agencies (Switzerland); MST (Taipei); ThEPCenter, IPST, STAR, and NSTDA (Thailand); TUBITAK and TAEK (Turkey); NASU and SFFR (Ukraine); STFC (United Kingdom); DOE and NSF (USA).

Individuals have received support from the Marie-Curie programme and the European Research Council and EPLANET (European Union); the Leventis Foundation; the A. P. Sloan Foundation; the Alexander von Humboldt Foundation; the Belgian Federal Science Policy Office; the Fonds pour la Formation à la Recherche dans l'Industrie et dans l'Agriculture (FRIA-Belgium); the Agentschap voor Innovatie door Wetenschap en Technologie (IWT-Belgium); the Ministry of Education, Youth and Sports (MEYS) of the Czech Republic; the Council of Science and Industrial Research, India; the HOMING PLUS programme of the Foundation for Polish Science, cofinanced from European Union, Regional Development Fund, the Mobility Plus programme of the Ministry of Science and Higher Education, the National Science Center (Poland), contracts Harmonia 2014/14/M/ST2/00428, Opus 2014/13/B/ST2/02543, 2014/15/B/ST2/03998, and 2015/19/B/ST2/02861, Sonata-bis 2012/07/E/ST2/01406; the Thalís and Aristeia programmes cofinanced by EU-ESF and the Greek NSRF; the National Priorities Research Program by Qatar National Research Fund; the Programa Clarín-COFUND del Principado de Asturias; the Rachadapisek Sompot Fund for Postdoctoral Fellowship, Chulalongkorn University and the Chulalongkorn Academic into Its 2nd Century Project Advancement Project (Thailand); and the Welch Foundation, contract C-1845.

References

- [1] N. Arkani-Hamed, A. G. Cohen, and H. Georgi, "Electroweak symmetry breaking from dimensional deconstruction", *Phys. Lett. B* **513** (2001) 232, doi:10.1016/S0370-2693(01)00741-9, arXiv:hep-ph/0105239.
- [2] M. Schmaltz and D. Tucker-Smith, "Little Higgs review", *Ann. Rev. Nucl. Part. Sci.* **55** (2005) 229, doi:10.1146/annurev.nucl.55.090704.151502, arXiv:hep-ph/0502182.
- [3] M. Perelstein, M. E. Peskin, and A. Pierce, "Top quarks and electroweak symmetry breaking in little Higgs models", *Phys. Rev. D* **69** (2004) 075002, doi:10.1103/PhysRevD.69.075002, arXiv:hep-ph/0310039.
- [4] I. Antoniadis, K. Benakli, and M. Quiros, "Finite Higgs mass without supersymmetry", *New J. Phys.* **3** (2001) 20, doi:10.1088/1367-2630/3/1/320, arXiv:hep-th/0108005.
- [5] Y. Hosotani, S. Noda, and K. Takenaga, "Dynamical gauge-Higgs unification in the electroweak theory", *Phys. Lett. B* **607** (2005) 276, doi:10.1016/j.physletb.2004.12.029, arXiv:hep-ph/0410193.
- [6] M. J. Dugan, H. Georgi, and D. B. Kaplan, "Anatomy of a composite Higgs model", *Nucl. Phys. B* **254** (1985) 299, doi:10.1016/0550-3213(85)90221-4.
- [7] D. B. Kaplan, "Flavor at SSC energies: A new mechanism for dynamically generated fermion masses", *Nucl. Phys. B* **365** (1991) 259, doi:10.1016/S0550-3213(05)80021-5.

- [8] K. Agashe, R. Contino, and A. Pomarol, “The minimal composite Higgs model”, *Nucl. Phys. B* **719** (2005) 165, doi:10.1016/j.nuclphysb.2005.04.035, arXiv:hep-ph/0412089.
- [9] R. Contino, L. Da Rold, and A. Pomarol, “Light custodians in natural composite Higgs models”, *Phys. Rev. D* **75** (2007) 055014, doi:10.1103/PhysRevD.75.055014, arXiv:hep-ph/0612048.
- [10] A. De Simone, O. Matsedonskyi, R. Rattazzi, and A. Wulzer, “A first top partner hunter’s guide”, *JHEP* **04** (2013) 1, doi:10.1007/JHEP04(2013)004, arXiv:1211.5663.
- [11] ATLAS Collaboration, “Observation of a new particle in the search for the Standard Model Higgs boson with the ATLAS detector at the LHC”, *Phys. Lett. B* **716** (2012) 1, doi:10.1016/j.physletb.2012.08.020, arXiv:1207.7214.
- [12] CMS Collaboration, “Observation of a new boson at a mass of 125 GeV with the CMS experiment at the LHC”, *Phys. Lett. B* **716** (2012) 30, doi:10.1016/j.physletb.2012.08.021, arXiv:1207.7235.
- [13] CMS Collaboration, “Observation of a new boson with mass near 125 GeV in pp collisions at $\sqrt{s} = 7$ and 8 TeV”, *JHEP* **06** (2013) 081, doi:10.1007/JHEP06(2013)081, arXiv:1303.4571.
- [14] O. Eberhardt et al., “Joint analysis of Higgs boson decays and electroweak precision observables in the standard model with a sequential fourth generation”, *Phys. Rev. D* **86** (2012) 013011, doi:10.1103/PhysRevD.86.013011, arXiv:1204.3872.
- [15] J. A. Aguilar-Saavedra, R. Benbrik, S. Heinemeyer, and M. Pérez-Victoria, “Handbook of vector-like quarks: mixing and single production”, *Phys. Rev. D* **88** (2013) 094010, doi:10.1103/PhysRevD.88.094010, arXiv:1306.0572.
- [16] ATLAS Collaboration, “Search for pair and single production of new heavy quarks that decay to a Z boson and a third-generation quark in pp collisions at $\sqrt{s} = 8$ TeV with the ATLAS detector”, *JHEP* **11** (2014) 104, doi:10.1007/JHEP11(2014)104, arXiv:1409.5500.
- [17] ATLAS Collaboration, “Analysis of events with b-jets and a pair of leptons of the same charge in pp collisions at $\sqrt{s} = 8$ TeV with the ATLAS detector”, *JHEP* **10** (2015) 150, doi:10.1007/JHEP10(2015)150, arXiv:1504.04605.
- [18] ATLAS Collaboration, “Search for production of vector-like quark pairs and of four top quarks in the lepton-plus-jets final state in pp collisions at $\sqrt{s} = 8$ TeV with the ATLAS detector”, *JHEP* **08** (2015) 105, doi:10.1007/JHEP08(2015)105, arXiv:1505.04306.
- [19] ATLAS Collaboration, “Search for the production of single vector-like and excited quarks in the Wt final state in pp collisions at $\sqrt{s} = 8$ TeV with the ATLAS detector”, *JHEP* **02** (2016) 110, doi:10.1007/JHEP02(2016)110, arXiv:1510.02664.
- [20] ATLAS Collaboration, “Search for single production of vector-like quarks decaying into Wb in pp collisions at $\sqrt{s} = 8$ TeV with the ATLAS detector”, *Eur. Phys. J. C* **76** (2016), no. 8, 442, doi:10.1140/epjc/s10052-016-4281-8, arXiv:1602.05606.

- [21] CMS Collaboration, “Search for vector-like charge $2/3$ T quarks in proton-proton collisions at $\sqrt{s} = 8$ TeV”, *Phys. Rev. D* **93** (2016) 012003, doi:10.1103/PhysRevD.93.012003, arXiv:1509.04177.
- [22] CMS Collaboration, “Search for vector-like T quarks decaying to top quarks and Higgs bosons in the all-hadronic channel using jet substructure”, *JHEP* **06** (2015) 080, doi:10.1007/JHEP06(2015)080, arXiv:1503.01952.
- [23] O. Matsedonskyi, G. Panico, and A. Wulzer, “On the interpretation of top partners searches”, *JHEP* **12** (2014) 097, doi:10.1007/JHEP12(2014)097, arXiv:1409.0100.
- [24] CMS Collaboration, “The CMS experiment at the CERN LHC”, *JINST* **3** (2008) S08004, doi:10.1088/1748-0221/3/08/S08004.
- [25] CMS Collaboration, “Particle-flow event reconstruction in CMS and performance for jets, taus, and E_T^{miss} ”, CMS Physics Analysis Summary CMS-PAS-PFT-09-001, 2009.
- [26] CMS Collaboration, “Commissioning of the particle-flow event with the first LHC collisions recorded in the CMS detector”, CMS Physics Analysis Summary CMS-PAS-PFT-10-001, 2010.
- [27] CMS Collaboration, “Performance of electron reconstruction and selection with the CMS detector in proton-proton collisions at $\sqrt{s} = 8$ TeV”, *JINST* **10** (2015) P06005, doi:10.1088/1748-0221/10/06/P06005, arXiv:1502.02701.
- [28] CMS Collaboration, “Performance of CMS muon reconstruction in pp collision events at $\sqrt{s} = 7$ TeV”, *JINST* **7** (2012) P10002, doi:10.1088/1748-0221/7/10/P10002, arXiv:1206.4071.
- [29] M. Cacciari, G. P. Salam, and G. Soyez, “The anti- k_t jet clustering algorithm”, *JHEP* **04** (2008) 063, doi:10.1088/1126-6708/2008/04/063, arXiv:0802.1189.
- [30] M. Cacciari, G. P. Salam, and G. Soyez, “FastJet user manual”, *Eur. Phys. J. C* **72** (2012) 1896, doi:10.1140/epjc/s10052-012-1896-2, arXiv:1111.6097.
- [31] M. Cacciari, G. P. Salam, and G. Soyez, “The catchment area of jets”, *JHEP* **04** (2008) 005, doi:10.1088/1126-6708/2008/04/005, arXiv:0802.1188.
- [32] CMS Collaboration, “Determination of jet energy calibration and transverse momentum resolution in CMS”, *JINST* **6** (2011) P11002, doi:10.1088/1748-0221/6/11/P11002, arXiv:1107.4277.
- [33] CMS Collaboration, “Identification of b-quark jets with the CMS experiment”, *JINST* **8** (2013) P04013, doi:10.1088/1748-0221/8/04/P04013, arXiv:1211.4462.
- [34] J. Alwall et al., “The automated computation of tree-level and next-to-leading order differential cross sections, and their matching to parton shower simulations”, *JHEP* **07** (2014) 079, doi:10.1007/JHEP07(2014)079, arXiv:1405.0301.
- [35] P. Nason, “A new method for combining NLO QCD with shower Monte Carlo algorithms”, *JHEP* **11** (2004) 040, doi:10.1088/1126-6708/2004/11/040, arXiv:hep-ph/0409146.

- [36] S. Frixione, P. Nason, and C. Oleari, “Matching NLO QCD computations with parton shower simulations: the POWHEG method”, *JHEP* **11** (2007) 070, doi:10.1088/1126-6708/2007/11/070, arXiv:0709.2092.
- [37] S. Alioli, P. Nason, C. Oleari, and E. Re, “A general framework for implementing NLO calculations in shower Monte Carlo programs: the POWHEG BOX”, *JHEP* **06** (2010) 043, doi:10.1007/JHEP06(2010)043, arXiv:1002.2581.
- [38] S. Frixione, P. Nason, and G. Ridolfi, “A positive-weight next-to-leading-order Monte Carlo for heavy flavour hadroproduction”, *JHEP* **09** (2007) 126, doi:10.1088/1126-6708/2007/09/126, arXiv:0707.3088.
- [39] M. L. Mangano, M. Moretti, F. Piccinini, and M. Treccani, “Matching matrix elements and shower evolution for top-pair production in hadronic collisions”, *JHEP* **01** (2007) 013, doi:10.1088/1126-6708/2007/01/013, arXiv:hep-ph/0611129.
- [40] T. Sjöstrand, S. Mrenna, and P. Skands, “PYTHIA 6.4 physics and manual”, *JHEP* **05** (2006) 026, doi:10.1088/1126-6708/2006/05/026, arXiv:hep-ph/0603175.
- [41] T. Sjöstrand et al., “An Introduction to PYTHIA 8.2”, *Comput. Phys. Commun.* **191** (2015) 159, doi:10.1016/j.cpc.2015.01.024, arXiv:1410.3012.
- [42] CMS Collaboration, “Event generator tunes obtained from underlying event and multiparton scattering measurements”, *Eur. Phys. J. C* **76** (2016) 1, doi:10.1140/epjc/s10052-016-3988-x.
- [43] NNPDF Collaboration, “Parton distributions for the LHC Run II”, *JHEP* **04** (2015) 040, doi:10.1007/JHEP04(2015)040, arXiv:1410.8849.
- [44] GEANT4 Collaboration, “GEANT4—a simulation toolkit”, *Nucl. Instrum. Meth. A* **506** (2003) 250, doi:10.1016/S0168-9002(03)01368-8.
- [45] J. Allison et al., “GEANT4 developments and applications”, *IEEE Trans. Nucl. Sci.* **53** (2006) 270, doi:10.1109/TNS.2006.869826.
- [46] CMS Collaboration, “Description and performance of track and primary-vertex reconstruction with the CMS tracker”, *JINST* **9** (2014) P10009, doi:10.1088/1748-0221/9/10/P10009, arXiv:1405.6569.
- [47] W. Waltenberger, R. Frühwirth, and P. Vanlaer, “Adaptive Vertex Fitting”, *J. Phys. G* **34** (2007) N343, doi:10.1088/0954-3899/34/12/N01.
- [48] M. Dasgupta, A. Fregoso, S. Marzani, and G. P. Salam, “Towards an understanding of jet substructure”, *JHEP* **09** (2013) 029, doi:10.1007/JHEP09(2013)029, arXiv:1307.0007.
- [49] A. J. Larkoski, S. Marzani, G. Soyez, and J. Thaler, “Soft drop”, *JHEP* **05** (2014) 146, doi:10.1007/JHEP05(2014)146, arXiv:1402.2657.
- [50] J. Thaler and K. Van Tilburg, “Maximizing boosted top identification by minimizing N-subjettiness”, *JHEP* **02** (2012) 093, doi:10.1007/JHEP02(2012)093, arXiv:1108.2701.
- [51] J. Thaler and K. Van Tilburg, “Identifying boosted objects with N-subjettiness”, *JHEP* **03** (2011) 015, doi:10.1007/JHEP03(2011)015, arXiv:1011.2268.

- [52] Particle Data Group Collaboration, “Review of Particle Physics”, *Chin. Phys. C* **38** (2014) 090001, doi:10.1088/1674-1137/38/9/090001.
- [53] N. D. Gagunashvili, “Pearson’s Chi-Square Test Modifications for Comparison of Unweighted and Weighted Histograms and Two Weighted Histograms”, in *XI International Workshop on Advanced Computing and Analysis Techniques in Physics Research*. SISSA, 2007. arXiv:physics/0605123. PoS(ACAT)060.
- [54] ATLAS Collaboration, “Measurement of the Inelastic Proton-Proton Cross Section at $\sqrt{s} = 13$ TeV with the ATLAS Detector at the LHC”, *Phys. Rev. Lett.* (2016), no. 117, 182002, doi:10.1103/PhysRevLett.117.182002, arXiv:1606.02625.
- [55] CMS Collaboration, “CMS Luminosity Measurement for the 2015 Data Taking Period”, CMS Physics Analysis Summary CMS-PAS-LUM-15-001, 2016.
- [56] J. Butterworth et al., “PDF4LHC recommendations for LHC Run II”, *J. Phys. G* **43** (2016) 023001, doi:10.1088/0954-3899/43/2/023001, arXiv:1510.03865.
- [57] T. Müller, J. Ott, and J. Wagner-Kuhr, “theta – a framework for template-based modeling and inference”, 2010.
- [58] A. O’Hagan and J. J. Forster, “Kendall’s Advanced Theory of Statistics. Vol. 2B: Bayesian Inference”. Arnold, London, 2004.
- [59] R. J. Barlow and C. Beeston, “Fitting using finite Monte Carlo samples”, *Comput. Phys. Commun.* **77** (1993) 219, doi:10.1016/0010-4655(93)90005-W.
- [60] J. Campbell, R. K. Ellis, and F. Tramontano, “Single top-quark production and decay at next-to-leading order”, *Phys. Rev. D* **70** (2004) 094012, doi:10.1103/PhysRevD.70.094012, arXiv:hep-ph/0408180.

A The CMS Collaboration

Yerevan Physics Institute, Yerevan, Armenia

V. Khachatryan, A.M. Sirunyan, A. Tumasyan

Institut für Hochenergiephysik, Wien, Austria

W. Adam, E. Asilar, T. Bergauer, J. Brandstetter, E. Brondolin, M. Dragicevic, J. Erö, M. Flechl, M. Friedl, R. Frühwirth¹, V.M. Ghete, C. Hartl, N. Hörmann, J. Hrubec, M. Jeitler¹, A. König, I. Krätschmer, D. Liko, T. Matsushita, I. Mikulec, D. Rabady, N. Rad, B. Rahbaran, H. Rohringer, J. Schieck¹, J. Strauss, W. Waltenberger, C.-E. Wulz¹

Institute for Nuclear Problems, Minsk, Belarus

O. Dvornikov, V. Makarenko, V. Zykunov

National Centre for Particle and High Energy Physics, Minsk, Belarus

V. Mossolov, N. Shumeiko, J. Suarez Gonzalez

Universiteit Antwerpen, Antwerpen, Belgium

S. Alderweireldt, E.A. De Wolf, X. Janssen, J. Lauwers, M. Van De Klundert, H. Van Haevermaet, P. Van Mechelen, N. Van Remortel, A. Van Spilbeek

Vrije Universiteit Brussel, Brussel, Belgium

S. Abu Zeid, F. Blekman, J. D'Hondt, N. Daci, I. De Bruyn, K. Deroover, S. Lowette, S. Moortgat, L. Moreels, A. Olbrechts, Q. Python, S. Tavernier, W. Van Doninck, P. Van Mulders, I. Van Parijs

Université Libre de Bruxelles, Bruxelles, Belgium

H. Brun, B. Clerbaux, G. De Lentdecker, H. Delannoy, G. Fasanella, L. Favart, R. Goldouzian, A. Grebenyuk, G. Karapostoli, T. Lenzi, A. Léonard, J. Luetic, T. Maerschalk, A. Marinov, A. Randle-conde, T. Seva, C. Vander Velde, P. Vanlaer, D. Vannerom, R. Yonamine, F. Zenoni, F. Zhang²

Ghent University, Ghent, Belgium

A. Cimmino, T. Cornelis, D. Dobur, A. Fagot, G. Garcia, M. Gul, I. Khvastunov, D. Poyraz, S. Salva, R. Schöfbeck, A. Sharma, M. Tytgat, W. Van Driessche, E. Yazgan, N. Zaganidis

Université Catholique de Louvain, Louvain-la-Neuve, Belgium

H. Bakhshiansohi, C. Beluffi³, O. Bondu, S. Brochet, G. Bruno, A. Caudron, S. De Visscher, C. Delaere, M. Delcourt, B. Francois, A. Giammanco, A. Jafari, P. Jez, M. Komm, G. Krintiras, V. Lemaitre, A. Magitteri, A. Mertens, M. Musich, C. Nuttens, K. Piotrkowski, L. Quertenmont, M. Selvaggi, M. Vidal Marono, S. Wertz

Université de Mons, Mons, Belgium

N. Beliy

Centro Brasileiro de Pesquisas Fisicas, Rio de Janeiro, Brazil

W.L. Aldá Júnior, F.L. Alves, G.A. Alves, L. Brito, C. Hensel, A. Moraes, M.E. Pol, P. Rebello Teles

Universidade do Estado do Rio de Janeiro, Rio de Janeiro, Brazil

E. Belchior Batista Das Chagas, W. Carvalho, J. Chinellato⁴, A. Custódio, E.M. Da Costa, G.G. Da Silveira⁵, D. De Jesus Damiao, C. De Oliveira Martins, S. Fonseca De Souza, L.M. Huertas Guativa, H. Malbouisson, D. Matos Figueiredo, C. Mora Herrera, L. Mundim, H. Nogima, W.L. Prado Da Silva, A. Santoro, A. Sznajder, E.J. Tonelli Manganote⁴, A. Vilela Pereira

Universidade Estadual Paulista ^a, Universidade Federal do ABC ^b, São Paulo, Brazil

S. Ahuja^a, C.A. Bernardes^b, S. Dogra^a, T.R. Fernandez Perez Tomei^a, E.M. Gregores^b, P.G. Mercadante^b, C.S. Moon^a, S.F. Novaes^a, Sandra S. Padula^a, D. Romero Abad^b, J.C. Ruiz Vargas

Institute for Nuclear Research and Nuclear Energy, Sofia, Bulgaria

A. Aleksandrov, R. Hadjiiska, P. Iaydjiev, M. Rodozov, S. Stoykova, G. Sultanov, M. Vutova

University of Sofia, Sofia, Bulgaria

A. Dimitrov, I. Glushkov, L. Litov, B. Pavlov, P. Petkov

Beihang University, Beijing, China

W. Fang⁶

Institute of High Energy Physics, Beijing, China

M. Ahmad, J.G. Bian, G.M. Chen, H.S. Chen, M. Chen, Y. Chen⁷, T. Cheng, C.H. Jiang, D. Leggat, Z. Liu, F. Romeo, S.M. Shaheen, A. Spiezia, J. Tao, C. Wang, Z. Wang, H. Zhang, J. Zhao

State Key Laboratory of Nuclear Physics and Technology, Peking University, Beijing, China

Y. Ban, G. Chen, Q. Li, S. Liu, Y. Mao, S.J. Qian, D. Wang, Z. Xu

Universidad de Los Andes, Bogota, Colombia

C. Avila, A. Cabrera, L.F. Chaparro Sierra, C. Florez, J.P. Gomez, C.F. González Hernández, J.D. Ruiz Alvarez, J.C. Sanabria

University of Split, Faculty of Electrical Engineering, Mechanical Engineering and Naval Architecture, Split, Croatia

N. Godinovic, D. Lelas, I. Puljak, P.M. Ribeiro Cipriano, T. Sculac

University of Split, Faculty of Science, Split, Croatia

Z. Antunovic, M. Kovac

Institute Rudjer Boskovic, Zagreb, Croatia

V. Brigljevic, D. Ferencek, K. Kadija, S. Micanovic, L. Sudic, T. Susa

University of Cyprus, Nicosia, Cyprus

A. Attikis, G. Mavromanolakis, J. Mousa, C. Nicolaou, F. Ptochos, P.A. Razis, H. Rykaczewski, D. Tsiakkouri

Charles University, Prague, Czech Republic

M. Finger⁸, M. Finger Jr.⁸

Universidad San Francisco de Quito, Quito, Ecuador

E. Carrera Jarrin

Academy of Scientific Research and Technology of the Arab Republic of Egypt, Egyptian Network of High Energy Physics, Cairo, Egypt

Y. Assran^{9,10}, T. Elkafrawy¹¹, A. Mahrous¹²

National Institute of Chemical Physics and Biophysics, Tallinn, Estonia

B. Calpas, M. Kadastik, M. Murumaa, L. Perrini, M. Raidal, A. Tiko, C. Veelken

Department of Physics, University of Helsinki, Helsinki, Finland

P. Eerola, J. Pekkanen, M. Voutilainen

Helsinki Institute of Physics, Helsinki, Finland

J. Härkönen, T. Järvinen, V. Karimäki, R. Kinnunen, T. Lampén, K. Lassila-Perini, S. Lehti, T. Lindén, P. Luukka, J. Tuominiemi, E. Tuovinen, L. Wendland

Lappeenranta University of Technology, Lappeenranta, Finland

J. Talvitie, T. Tuuva

IRFU, CEA, Université Paris-Saclay, Gif-sur-Yvette, France

M. Besancon, F. Couderc, M. Dejardin, D. Denegri, B. Fabbro, J.L. Faure, C. Favaro, F. Ferri, S. Ganjour, S. Ghosh, A. Givernaud, P. Gras, G. Hamel de Monchenault, P. Jarry, I. Kucher, E. Locci, M. Machet, J. Malcles, J. Rander, A. Rosowsky, M. Titov, A. Zghiche

Laboratoire Leprince-Ringuet, Ecole Polytechnique, IN2P3-CNRS, Palaiseau, France

A. Abdulsalam, I. Antropov, S. Baffioni, F. Beaudette, P. Busson, L. Cadamuro, E. Chapon, C. Charlot, O. Davignon, R. Granier de Cassagnac, M. Jo, S. Lisniak, P. Miné, M. Nguyen, C. Ochando, G. Ortona, P. Paganini, P. Pigard, S. Regnard, R. Salerno, Y. Sirois, T. Strebler, Y. Yilmaz, A. Zabi

Institut Pluridisciplinaire Hubert Curien, Université de Strasbourg, Université de Haute Alsace Mulhouse, CNRS/IN2P3, Strasbourg, France

J.-L. Agram¹³, J. Andrea, A. Aubin, D. Bloch, J.-M. Brom, M. Buttignol, E.C. Chabert, N. Chanon, C. Collard, E. Conte¹³, X. Coubez, J.-C. Fontaine¹³, D. Gelé, U. Goerlach, A.-C. Le Bihan, K. Skovpen, P. Van Hove

Centre de Calcul de l'Institut National de Physique Nucleaire et de Physique des Particules, CNRS/IN2P3, Villeurbanne, France

S. Gadrat

Université de Lyon, Université Claude Bernard Lyon 1, CNRS-IN2P3, Institut de Physique Nucléaire de Lyon, Villeurbanne, France

S. Beauceron, C. Bernet, G. Boudoul, E. Bouvier, C.A. Carrillo Montoya, R. Chierici, D. Contardo, B. Courbon, P. Depasse, H. El Mamouni, J. Fan, J. Fay, S. Gascon, M. Gouzevitch, G. Grenier, B. Ille, F. Lagarde, I.B. Laktineh, M. Lethuillier, L. Mirabito, A.L. Pequegnot, S. Perries, A. Popov¹⁴, D. Sabes, V. Sordini, M. Vander Donckt, P. Verdier, S. Viret

Georgian Technical University, Tbilisi, Georgia

T. Toriashvili¹⁵

Tbilisi State University, Tbilisi, Georgia

Z. Tsamalaidze⁸

RWTH Aachen University, I. Physikalisches Institut, Aachen, Germany

C. Autermann, S. Beranek, L. Feld, A. Heister, M.K. Kiesel, K. Klein, M. Lipinski, A. Ostapchuk, M. Preuten, F. Raupach, S. Schael, C. Schomakers, J. Schulz, T. Verlage, H. Weber, V. Zhukov¹⁴

RWTH Aachen University, III. Physikalisches Institut A, Aachen, Germany

A. Albert, M. Brodski, E. Dietz-Laursonn, D. Duchardt, M. Endres, M. Erdmann, S. Erdweg, T. Esch, R. Fischer, A. Güth, M. Hamer, T. Hebbeker, C. Heidemann, K. Hoepfner, S. Knutzen, M. Merschmeyer, A. Meyer, P. Millet, S. Mukherjee, M. Olschewski, K. Padeken, T. Pook, M. Radziej, H. Reithler, M. Rieger, F. Scheuch, L. Sonnenschein, D. Teyssier, S. Thüer

RWTH Aachen University, III. Physikalisches Institut B, Aachen, Germany

V. Cherepanov, G. Flügge, F. Hoehle, B. Kargoll, T. Kress, A. Künsken, J. Lingemann, T. Müller, A. Nehr Korn, A. Nowack, I.M. Nugent, C. Pistone, O. Pooth, A. Stahl¹⁶

Deutsches Elektronen-Synchrotron, Hamburg, Germany

M. Aldaya Martin, T. Arndt, C. Asawatangtrakuldee, K. Beernaert, O. Behnke, U. Behrens, A.A. Bin Anuar, K. Borras¹⁷, A. Campbell, P. Connor, C. Contreras-Campana, F. Costanza, C. Diez Pardos, G. Dolinska, G. Eckerlin, D. Eckstein, T. Eichhorn, E. Eren, E. Gallo¹⁸, J. Garay Garcia, A. Geiser, A. Gizhko, J.M. Grados Luyando, P. Gunnellini, A. Harb, J. Hauk, M. Hempel¹⁹, H. Jung, A. Kalogeropoulos, O. Karacheban¹⁹, M. Kasemann, J. Keaveney, C. Kleinwort, I. Korol, D. Krücker, W. Lange, A. Lelek, J. Leonard, K. Lipka, A. Lobanov, W. Lohmann¹⁹, R. Mankel, I.-A. Melzer-Pellmann, A.B. Meyer, G. Mittag, J. Mnich, A. Mussgiller, E. Ntomari, D. Pitzl, R. Placakyte, A. Raspereza, B. Roland, M.Ö. Sahin, P. Saxena, T. Schoerner-Sadenius, C. Seitz, S. Spannagel, N. Stefaniuk, G.P. Van Onsem, R. Walsh, C. Wissing

University of Hamburg, Hamburg, Germany

V. Blobel, M. Centis Vignali, A.R. Draeger, T. Dreyer, E. Garutti, D. Gonzalez, J. Haller, M. Hoffmann, A. Junkes, R. Klanner, R. Kogler, N. Kovalchuk, T. Lapsien, T. Lenz, I. Marchesini, D. Marconi, M. Meyer, M. Niedziela, D. Nowatschin, F. Pantaleo¹⁶, T. Peiffer, A. Perieanu, J. Poehlsen, C. Sander, C. Scharf, P. Schleper, A. Schmidt, S. Schumann, J. Schwandt, H. Stadie, G. Steinbrück, F.M. Stober, M. Stöver, H. Tholen, D. Troendle, E. Usai, L. Vanelderden, A. Vanhoefer, B. Vormwald

Institut für Experimentelle Kernphysik, Karlsruhe, Germany

M. Akbiyik, C. Barth, S. Baur, C. Baus, J. Berger, E. Butz, R. Caspart, T. Chwalek, F. Colombo, W. De Boer, A. Dierlamm, S. Fink, B. Freund, R. Friese, M. Giffels, A. Gilbert, P. Goldenzweig, D. Haitz, F. Hartmann¹⁶, S.M. Heindl, U. Husemann, I. Katkov¹⁴, S. Kudella, P. Lobelle Pardo, H. Mildner, M.U. Mozer, Th. Müller, M. Plagge, G. Quast, K. Rabbertz, S. Röcker, F. Roscher, M. Schröder, I. Shvetsov, G. Sieber, H.J. Simonis, R. Ulrich, J. Wagner-Kuhr, S. Wayand, M. Weber, T. Weiler, S. Williamson, C. Wöhrmann, R. Wolf

Institute of Nuclear and Particle Physics (INPP), NCSR Demokritos, Aghia Paraskevi, Greece

G. Anagnostou, G. Daskalakis, T. Gerasis, V.A. Giakoumopoulou, A. Kyriakis, D. Loukas, I. Topsis-Giotis

National and Kapodistrian University of Athens, Athens, Greece

S. Kesisoglou, A. Panagiotou, N. Saoulidou, E. Tziaferi

University of Ioánnina, Ioánnina, Greece

I. Evangelou, G. Flouris, C. Foudas, P. Kokkas, N. Loukas, N. Manthos, I. Papadopoulos, E. Paradas

MTA-ELTE Lendület CMS Particle and Nuclear Physics Group, Eötvös Loránd University, Budapest, Hungary

N. Filipovic

Wigner Research Centre for Physics, Budapest, Hungary

G. Bencze, C. Hajdu, P. Hidas, D. Horvath²⁰, F. Sikler, V. Veszpremi, G. Vesztergombi²¹, A.J. Zsigmond

Institute of Nuclear Research ATOMKI, Debrecen, Hungary

N. Beni, S. Czellar, J. Karancsi²², A. Makovec, J. Molnar, Z. Szillasi

Institute of Physics, University of Debrecen

M. Bartók²¹, P. Raics, Z.L. Trocsanyi, B. Ujvari

National Institute of Science Education and Research, Bhubaneswar, India

S. Bahinipati, S. Choudhury²³, P. Mal, K. Mandal, A. Nayak²⁴, D.K. Sahoo, N. Sahoo, S.K. Swain

Panjab University, Chandigarh, India

S. Bansal, S.B. Beri, V. Bhatnagar, R. Chawla, U. Bhawandeep, A.K. Kalsi, A. Kaur, M. Kaur, R. Kumar, P. Kumari, A. Mehta, M. Mittal, J.B. Singh, G. Walia

University of Delhi, Delhi, India

Ashok Kumar, A. Bhardwaj, B.C. Choudhary, R.B. Garg, S. Keshri, S. Malhotra, M. Naimuddin, N. Nishu, K. Ranjan, R. Sharma, V. Sharma

Saha Institute of Nuclear Physics, Kolkata, India

R. Bhattacharya, S. Bhattacharya, K. Chatterjee, S. Dey, S. Dutt, S. Dutta, S. Ghosh, N. Majumdar, A. Modak, K. Mondal, S. Mukhopadhyay, S. Nandan, A. Purohit, A. Roy, D. Roy, S. Roy Chowdhury, S. Sarkar, M. Sharan, S. Thakur

Indian Institute of Technology Madras, Madras, India

P.K. Behera

Bhabha Atomic Research Centre, Mumbai, India

R. Chudasama, D. Dutta, V. Jha, V. Kumar, A.K. Mohanty¹⁶, P.K. Netrakanti, L.M. Pant, P. Shukla, A. Topkar

Tata Institute of Fundamental Research-A, Mumbai, India

T. Aziz, S. Dugad, G. Kole, B. Mahakud, S. Mitra, G.B. Mohanty, B. Parida, N. Sur, B. Sutar

Tata Institute of Fundamental Research-B, Mumbai, India

S. Banerjee, S. Bhowmik²⁵, R.K. Dewanjee, S. Ganguly, M. Guchait, Sa. Jain, S. Kumar, M. Maity²⁵, G. Majumder, K. Mazumdar, T. Sarkar²⁵, N. Wickramage²⁶

Indian Institute of Science Education and Research (IISER), Pune, India

S. Chauhan, S. Dube, V. Hegde, A. Kapoor, K. Kothekar, S. Pandey, A. Rane, S. Sharma

Institute for Research in Fundamental Sciences (IPM), Tehran, Iran

H. Behnamian, S. Chenarani²⁷, E. Eskandari Tadavani, S.M. Etesami²⁷, A. Fahim²⁸, M. Khakzad, M. Mohammadi Najafabadi, M. Naseri, S. Paktinat Mehdiabadi²⁹, F. Rezaei Hosseinabadi, B. Safarzadeh³⁰, M. Zeinali

University College Dublin, Dublin, Ireland

M. Felcini, M. Grunewald

INFN Sezione di Bari ^a, Università di Bari ^b, Politecnico di Bari ^c, Bari, Italy

M. Abbrescia^{a,b}, C. Calabria^{a,b}, C. Caputo^{a,b}, A. Colaleo^a, D. Creanza^{a,c}, L. Cristella^{a,b}, N. De Filippis^{a,c}, M. De Palma^{a,b}, L. Fiore^a, G. Iaselli^{a,c}, G. Maggi^{a,c}, M. Maggi^a, G. Miniello^{a,b}, S. My^{a,b}, S. Nuzzo^{a,b}, A. Pompili^{a,b}, G. Pugliese^{a,c}, R. Radogna^{a,b}, A. Ranieri^a, G. Selvaggi^{a,b}, L. Silvestris^{a,16}, R. Venditti^{a,b}, P. Verwilligen^a

INFN Sezione di Bologna ^a, Università di Bologna ^b, Bologna, Italy

G. Abbiendi^a, C. Battilana, D. Bonacorsi^{a,b}, S. Braibant-Giacomelli^{a,b}, L. Brigliadori^{a,b}, R. Campanini^{a,b}, P. Capiluppi^{a,b}, A. Castro^{a,b}, F.R. Cavallo^a, S.S. Chhibra^{a,b}, G. Codispoti^{a,b}, M. Cuffiani^{a,b}, G.M. Dallavalle^a, F. Fabbri^a, A. Fanfani^{a,b}, D. Fasanella^{a,b}, P. Giacomelli^a, C. Grandi^a, L. Guiducci^{a,b}, S. Marcellini^a, G. Masetti^a, A. Montanari^a, F.L. Navarria^{a,b}, A. Perrotta^a, A.M. Rossi^{a,b}, T. Rovelli^{a,b}, G.P. Siroli^{a,b}, N. Tosi^{a,b,16}

INFN Sezione di Catania ^a, Università di Catania ^b, Catania, Italy

S. Albergo^{a,b}, M. Chiorboli^{a,b}, S. Costa^{a,b}, A. Di Mattia^a, F. Giordano^{a,b}, R. Potenza^{a,b}, A. Tricomi^{a,b}, C. Tuve^{a,b}

INFN Sezione di Firenze ^a, Università di Firenze ^b, Firenze, Italy

G. Barbagli^a, V. Ciulli^{a,b}, C. Civinini^a, R. D'Alessandro^{a,b}, E. Focardi^{a,b}, V. Gori^{a,b}, P. Lenzi^{a,b}, M. Meschini^a, S. Paoletti^a, G. Sguazzoni^a, L. Viliani^{a,b,16}

INFN Laboratori Nazionali di Frascati, Frascati, Italy

L. Benussi, S. Bianco, F. Fabbri, D. Piccolo, F. Primavera¹⁶

INFN Sezione di Genova ^a, Università di Genova ^b, Genova, Italy

V. Calvelli^{a,b}, F. Ferro^a, M. Lo Vetere^{a,b}, M.R. Monge^{a,b}, E. Robutti^a, S. Tosi^{a,b}

INFN Sezione di Milano-Bicocca ^a, Università di Milano-Bicocca ^b, Milano, Italy

L. Brianza¹⁶, M.E. Dinardo^{a,b}, S. Fiorendi^{a,b,16}, S. Gennai^a, A. Ghezzi^{a,b}, P. Govoni^{a,b}, M. Malberti, S. Malvezzi^a, R.A. Manzoni^{a,b,16}, D. Menasce^a, L. Moroni^a, M. Paganoni^{a,b}, D. Pedrini^a, S. Pigazzini, S. Ragazzi^{a,b}, T. Tabarelli de Fatis^{a,b}

INFN Sezione di Napoli ^a, Università di Napoli 'Federico II' ^b, Napoli, Italy, Università della Basilicata ^c, Potenza, Italy, Università G. Marconi ^d, Roma, Italy

S. Buontempo^a, N. Cavallo^{a,c}, G. De Nardo, S. Di Guida^{a,d,16}, M. Esposito^{a,b}, F. Fabozzi^{a,c}, F. Fienga^{a,b}, A.O.M. Iorio^{a,b}, G. Lanza^a, L. Lista^a, S. Meola^{a,d,16}, P. Paolucci^{a,16}, C. Sciacca^{a,b}, F. Thyssen

INFN Sezione di Padova ^a, Università di Padova ^b, Padova, Italy, Università di Trento ^c, Trento, Italy

P. Azzi^{a,16}, N. Bacchetta^a, L. Benato^{a,b}, D. Bisello^{a,b}, A. Boletti^{a,b}, R. Carlin^{a,b}, A. Carvalho Antunes De Oliveira^{a,b}, P. Checchia^a, M. Dall'Osso^{a,b}, P. De Castro Manzano^a, T. Dorigo^a, U. Dosselli^a, F. Gasparini^{a,b}, U. Gasparini^{a,b}, A. Gozzelino^a, S. Lacaprara^a, M. Margoni^{a,b}, A.T. Meneguzzo^{a,b}, J. Pazzini^{a,b}, N. Pozzobon^{a,b}, P. Ronchese^{a,b}, F. Simonetto^{a,b}, E. Torassa^a, M. Zanetti, P. Zotto^{a,b}, G. Zumerle^{a,b}

INFN Sezione di Pavia ^a, Università di Pavia ^b, Pavia, Italy

A. Braghieri^a, A. Magnani^{a,b}, P. Montagna^{a,b}, S.P. Ratti^{a,b}, V. Re^a, C. Riccardi^{a,b}, P. Salvini^a, I. Vai^{a,b}, P. Vitulo^{a,b}

INFN Sezione di Perugia ^a, Università di Perugia ^b, Perugia, Italy

L. Alunni Solestizi^{a,b}, G.M. Bilei^a, D. Ciangottini^{a,b}, L. Fanò^{a,b}, P. Lariccia^{a,b}, R. Leonardi^{a,b}, G. Mantovani^{a,b}, M. Menichelli^a, A. Saha^a, A. Santocchia^{a,b}

INFN Sezione di Pisa ^a, Università di Pisa ^b, Scuola Normale Superiore di Pisa ^c, Pisa, Italy

K. Androsov^{a,31}, P. Azzurri^{a,16}, G. Bagliesi^a, J. Bernardini^a, T. Boccali^a, R. Castaldi^a, M.A. Ciocci^{a,31}, R. Dell'Orso^a, S. Donato^{a,c}, G. Fedi, A. Giassi^a, M.T. Grippo^{a,31}, F. Ligabue^{a,c}, T. Lomtadze^a, L. Martini^{a,b}, A. Messineo^{a,b}, F. Palla^a, A. Rizzi^{a,b}, A. Savoy-Navarro^{a,32}, P. Spagnolo^a, R. Tenchini^a, G. Tonelli^{a,b}, A. Venturi^a, P.G. Verdini^a

INFN Sezione di Roma ^a, Università di Roma ^b, Roma, Italy

L. Barone^{a,b}, F. Cavallari^a, M. Cipriani^{a,b}, D. Del Re^{a,b,16}, M. Diemoz^a, S. Gelli^{a,b}, E. Longo^{a,b}, F. Margaroli^{a,b}, B. Marzocchi^{a,b}, P. Meridiani^a, G. Organtini^{a,b}, R. Paramatti^a, F. Preiato^{a,b}, S. Rahatlou^{a,b}, C. Rovelli^a, F. Santanastasio^{a,b}

INFN Sezione di Torino ^a, Università di Torino ^b, Torino, Italy, Università del Piemonte Orientale ^c, Novara, Italy

N. Amapane^{a,b}, R. Arcidiacono^{a,c,16}, S. Argiro^{a,b}, M. Arneodo^{a,c}, N. Bartosik^a, R. Bellan^{a,b},

C. Biino^a, N. Cartiglia^a, F. Cenna^{a,b}, M. Costa^{a,b}, R. Covarelli^{a,b}, A. Degano^{a,b}, G. Dellacasa^a, N. Demaria^a, L. Finco^{a,b}, B. Kiani^{a,b}, C. Mariotti^a, S. Maselli^a, E. Migliore^{a,b}, V. Monaco^{a,b}, E. Monteil^{a,b}, M.M. Obertino^{a,b}, L. Pacher^{a,b}, N. Pastrone^a, M. Pelliccioni^a, G.L. Pinna Angioni^{a,b}, F. Ravera^{a,b}, A. Romero^{a,b}, M. Ruspa^{a,c}, R. Sacchi^{a,b}, V. Sola^a, A. Solano^{a,b}, A. Staiano^a, P. Traczyk^{a,b}

INFN Sezione di Trieste^a, Università di Trieste^b, Trieste, Italy
S. Belforte^a, M. Casarsa^a, F. Cossutti^a, G. Della Ricca^{a,b}, A. Zanetti^a

Kyungpook National University, Daegu, Korea

D.H. Kim, G.N. Kim, M.S. Kim, S. Lee, S.W. Lee, Y.D. Oh, S. Sekmen, D.C. Son, Y.C. Yang

Chonbuk National University, Jeonju, Korea

A. Lee

Chonnam National University, Institute for Universe and Elementary Particles, Kwangju, Korea

H. Kim

Hanyang University, Seoul, Korea

J.A. Brochero Cifuentes, T.J. Kim

Korea University, Seoul, Korea

S. Cho, S. Choi, Y. Go, D. Gyun, S. Ha, B. Hong, Y. Jo, Y. Kim, B. Lee, K. Lee, K.S. Lee, S. Lee, J. Lim, S.K. Park, Y. Roh

Seoul National University, Seoul, Korea

J. Almond, J. Kim, H. Lee, S.B. Oh, B.C. Radburn-Smith, S.h. Seo, U.K. Yang, H.D. Yoo, G.B. Yu

University of Seoul, Seoul, Korea

M. Choi, H. Kim, J.H. Kim, J.S.H. Lee, I.C. Park, G. Ryu, M.S. Ryu

Sungkyunkwan University, Suwon, Korea

Y. Choi, J. Goh, C. Hwang, J. Lee, I. Yu

Vilnius University, Vilnius, Lithuania

V. Dudenas, A. Juodagalvis, J. Vaitkus

National Centre for Particle Physics, Universiti Malaya, Kuala Lumpur, Malaysia

I. Ahmed, Z.A. Ibrahim, J.R. Komaragiri, M.A.B. Md Ali³³, F. Mohamad Idris³⁴, W.A.T. Wan Abdullah, M.N. Yusli, Z. Zolkapli

Centro de Investigacion y de Estudios Avanzados del IPN, Mexico City, Mexico

H. Castilla-Valdez, E. De La Cruz-Burelo, I. Heredia-De La Cruz³⁵, A. Hernandez-Almada, R. Lopez-Fernandez, R. Magaña Villalba, J. Mejia Guisao, A. Sanchez-Hernandez

Universidad Iberoamericana, Mexico City, Mexico

S. Carrillo Moreno, C. Oropeza Barrera, F. Vazquez Valencia

Benemerita Universidad Autonoma de Puebla, Puebla, Mexico

S. Carpinteyro, I. Pedraza, H.A. Salazar Ibarguen, C. Uribe Estrada

Universidad Autónoma de San Luis Potosí, San Luis Potosí, Mexico

A. Morelos Pineda

University of Auckland, Auckland, New Zealand

D. Krofcheck

University of Canterbury, Christchurch, New Zealand

P.H. Butler

National Centre for Physics, Quaid-I-Azam University, Islamabad, Pakistan

A. Ahmad, M. Ahmad, Q. Hassan, H.R. Hoorani, W.A. Khan, A. Saddique, M.A. Shah, M. Shoaib, M. Waqas

National Centre for Nuclear Research, Swierk, Poland

H. Bialkowska, M. Bluj, B. Boimska, T. Frueboes, M. Górski, M. Kazana, K. Nawrocki, K. Romanowska-Rybinska, M. Szleper, P. Zalewski

Institute of Experimental Physics, Faculty of Physics, University of Warsaw, Warsaw, Poland

K. Bunkowski, A. Byzuk³⁶, K. Doroba, A. Kalinowski, M. Konecki, J. Krolikowski, M. Misiura, M. Olszewski, M. Walczak

Laboratório de Instrumentação e Física Experimental de Partículas, Lisboa, Portugal

P. Bargassa, C. Beirão Da Cruz E Silva, A. Di Francesco, P. Faccioli, P.G. Ferreira Parracho, M. Gallinaro, J. Hollar, N. Leonardo, L. Lloret Iglesias, M.V. Nemallapudi, J. Rodrigues Antunes, J. Seixas, O. Toldaiev, D. Vadrucchio, J. Varela, P. Vischia

Joint Institute for Nuclear Research, Dubna, Russia

S. Afanasiev, M. Gavrilenko, I. Golutvin, I. Gorbunov, A. Kamenev, V. Karjavin, A. Lanev, A. Malakhov, V. Matveev^{37,38}, V. Palichik, V. Perelygin, M. Savina, S. Shmatov, S. Shulha, N. Skatchkov, V. Smirnov, N. Voytishin, A. Zarubin

Petersburg Nuclear Physics Institute, Gatchina (St. Petersburg), Russia

L. Chtchypounov, V. Golovtsov, Y. Ivanov, V. Kim³⁹, E. Kuznetsova⁴⁰, V. Murzin, V. Oreshkin, V. Sulimov, A. Vorobyev

Institute for Nuclear Research, Moscow, Russia

Yu. Andreev, A. Dermenev, S. Gninenko, N. Golubev, A. Karneyeu, M. Kirsanov, N. Krasnikov, A. Pashenkov, D. Tlisov, A. Toropin

Institute for Theoretical and Experimental Physics, Moscow, Russia

V. Epshteyn, V. Gavrillov, N. Lychkovskaya, V. Popov, I. Pozdnyakov, G. Safronov, A. Spiridonov, M. Toms, E. Vlasov, A. Zhokin

Moscow Institute of Physics and Technology, Moscow, Russia

A. Bylinkin³⁸

National Research Nuclear University 'Moscow Engineering Physics Institute' (MEPhI), Moscow, Russia

R. Chistov⁴¹, M. Danilov⁴¹, S. Polikarpov

P.N. Lebedev Physical Institute, Moscow, Russia

V. Andreev, M. Azarkin³⁸, I. Dremin³⁸, M. Kirakosyan, A. Leonidov³⁸, S.V. Rusakov, A. Terkulov

Skobeltsyn Institute of Nuclear Physics, Lomonosov Moscow State University, Moscow, Russia

A. Baskakov, A. Belyaev, E. Boos, V. Bunichev, M. Dubinin⁴², L. Dudko, A. Gribushin, V. Klyukhin, O. Kodolova, I. Lokhtin, I. Miagkov, S. Obraztsov, M. Perfilov, S. Petrushanko, V. Savrin

Novosibirsk State University (NSU), Novosibirsk, Russia

V. Blinov⁴³, Y. Skovpen⁴³, D. Shtol⁴³

State Research Center of Russian Federation, Institute for High Energy Physics, Protvino, Russia

I. Azhgirey, I. Bayshev, S. Bitioukov, D. Elumakhov, V. Kachanov, A. Kalinin, D. Konstantinov, V. Krychkin, V. Petrov, R. Ryutin, A. Sobol, S. Troshin, N. Tyurin, A. Uzunian, A. Volkov

University of Belgrade, Faculty of Physics and Vinca Institute of Nuclear Sciences, Belgrade, Serbia

P. Adzic⁴⁴, P. Cirkovic, D. Devetak, M. Dordevic, J. Milosevic, V. Rekovic

Centro de Investigaciones Energéticas Medioambientales y Tecnológicas (CIEMAT), Madrid, Spain

J. Alcaraz Maestre, M. Barrio Luna, E. Calvo, M. Cerrada, M. Chamizo Llatas, N. Colino, B. De La Cruz, A. Delgado Peris, A. Escalante Del Valle, C. Fernandez Bedoya, J.P. Fernández Ramos, J. Flix, M.C. Fouz, P. Garcia-Abia, O. Gonzalez Lopez, S. Goy Lopez, J.M. Hernandez, M.I. Josa, E. Navarro De Martino, A. Pérez-Calero Yzquierdo, J. Puerta Pelayo, A. Quintario Olmeda, I. Redondo, L. Romero, M.S. Soares

Universidad Autónoma de Madrid, Madrid, Spain

J.F. de Trocóniz, M. Missiroli, D. Moran

Universidad de Oviedo, Oviedo, Spain

J. Cuevas, J. Fernandez Menendez, I. Gonzalez Caballero, J.R. González Fernández, E. Palencia Cortezon, S. Sanchez Cruz, I. Suárez Andrés, J.M. Vizán Garcia

Instituto de Física de Cantabria (IFCA), CSIC-Universidad de Cantabria, Santander, Spain

I.J. Cabrillo, A. Calderon, J.R. Castiñeiras De Saa, E. Curras, M. Fernandez, J. Garcia-Ferrero, G. Gomez, A. Lopez Virto, J. Marco, C. Martinez Rivero, F. Matorras, J. Piedra Gomez, T. Rodrigo, A. Ruiz-Jimeno, L. Scodellaro, N. Trevisani, I. Vila, R. Vilar Cortabitarte

CERN, European Organization for Nuclear Research, Geneva, Switzerland

D. Abbaneo, E. Auffray, G. Auzinger, M. Bachtis, P. Baillon, A.H. Ball, D. Barney, P. Bloch, A. Bocci, A. Bonato, C. Botta, T. Camporesi, R. Castello, M. Cepeda, G. Cerminara, M. D'Alfonso, D. d'Enterria, A. Dabrowski, V. Daponte, A. David, M. De Gruttola, A. De Roeck, E. Di Marco⁴⁵, M. Dobson, B. Dorney, T. du Pree, D. Duggan, M. Dünser, N. Dupont, A. Elliott-Peisert, S. Fartoukh, G. Franzoni, J. Fulcher, W. Funk, D. Gigi, K. Gill, M. Girone, F. Glege, D. Gulhan, S. Gundacker, M. Guthoff, J. Hammer, P. Harris, J. Hegeman, V. Innocente, P. Janot, J. Kieseler, H. Kirschenmann, V. Knünz, A. Kornmayer¹⁶, M.J. Kortelainen, K. Kousouris, M. Krammer¹, C. Lange, P. Lecoq, C. Lourenço, M.T. Lucchini, L. Malgeri, M. Mannelli, A. Martelli, F. Meijers, J.A. Merlin, S. Mersi, E. Meschi, P. Milenovic⁴⁶, F. Moortgat, S. Morovic, M. Mulders, H. Neugebauer, S. Orfanelli, L. Orsini, L. Pape, E. Perez, M. Peruzzi, A. Petrilli, G. Petrucciani, A. Pfeiffer, M. Pierini, A. Racz, T. Reis, G. Rolandi⁴⁷, M. Rovere, M. Ruan, H. Sakulin, J.B. Sauvan, C. Schäfer, C. Schwick, M. Seidel, A. Sharma, P. Silva, P. Sphicas⁴⁸, J. Steggemann, M. Stoye, Y. Takahashi, M. Tosi, D. Treille, A. Triossi, A. Tsirou, V. Veckalns⁴⁹, G.I. Veres²¹, M. Verweij, N. Wardle, H.K. Wöhri, A. Zagozdzinska³⁶, W.D. Zeuner

Paul Scherrer Institut, Villigen, Switzerland

W. Bertl, K. Deiters, W. Erdmann, R. Horisberger, Q. Ingram, H.C. Kaestli, D. Kotlinski, U. Langenegger, T. Rohe

Institute for Particle Physics, ETH Zurich, Zurich, Switzerland

F. Bachmair, L. Bäni, L. Bianchini, B. Casal, G. Dissertori, M. Dittmar, M. Donegà, C. Grab, C. Heidegger, D. Hits, J. Hoss, G. Kasieczka, P. Lecomte[†], W. Lustermann, B. Mangano, M. Marionneau, P. Martinez Ruiz del Arbol, M. Masciovecchio, M.T. Meinhard, D. Meister,

F. Micheli, P. Musella, F. Nessi-Tedaldi, F. Pandolfi, J. Pata, F. Pauss, G. Perrin, L. Perrozzi, M. Quitnat, M. Rossini, M. Schönenberger, A. Starodumov⁵⁰, V.R. Tavolaro, K. Theofilatos, R. Wallny

Universität Zürich, Zurich, Switzerland

T.K. Aarrestad, C. AMSler⁵¹, L. Caminada, M.F. Canelli, A. De Cosa, C. Galloni, A. Hinzmann, T. Hreus, B. Kilminster, J. Ngadiuba, D. Pinna, G. Rauco, P. Robmann, D. Salerno, Y. Yang, A. Zucchetta

National Central University, Chung-Li, Taiwan

V. Candelise, T.H. Doan, Sh. Jain, R. Khurana, M. Konyushikhin, C.M. Kuo, W. Lin, Y.J. Lu, A. Pozdnyakov, S.S. Yu

National Taiwan University (NTU), Taipei, Taiwan

Arun Kumar, P. Chang, Y.H. Chang, Y.W. Chang, Y. Chao, K.F. Chen, P.H. Chen, C. Dietz, F. Fiori, W.-S. Hou, Y. Hsiung, Y.F. Liu, R.-S. Lu, M. Miñano Moya, E. Paganis, A. Psallidas, J.f. Tsai, Y.M. Tzeng

Chulalongkorn University, Faculty of Science, Department of Physics, Bangkok, Thailand

B. Asavapibhop, G. Singh, N. Srimanobhas, N. Suwonjandee

Cukurova University - Physics Department, Science and Art Faculty

A. Adiguzel, M.N. Bakirci⁵², S. Damarseckin, Z.S. Demiroglu, C. Dozen, E. Eskut, S. Girgis, G. Gokbulut, Y. Guler, I. Hos, E.E. Kangal⁵³, O. Kara, U. Kiminsu, M. Oglakci, G. Onengut⁵⁴, K. Ozdemir⁵⁵, S. Ozturk⁵², A. Polatoz, D. Sunar Cerci⁵⁶, S. Turkcapar, I.S. Zorbakir, C. Zorbilmez

Middle East Technical University, Physics Department, Ankara, Turkey

B. Bilin, S. Bilmis, B. Isildak⁵⁷, G. Karapinar⁵⁸, M. Yalvac, M. Zeyrek

Bogazici University, Istanbul, Turkey

E. Gülmez, M. Kaya⁵⁹, O. Kaya⁶⁰, E.A. Yetkin⁶¹, T. Yetkin⁶²

Istanbul Technical University, Istanbul, Turkey

A. Cakir, K. Cankocak, S. Sen⁶³

Institute for Scintillation Materials of National Academy of Science of Ukraine, Kharkov, Ukraine

B. Grynyov

National Scientific Center, Kharkov Institute of Physics and Technology, Kharkov, Ukraine

L. Levchuk, P. Sorokin

University of Bristol, Bristol, United Kingdom

R. Aggleton, F. Ball, L. Beck, J.J. Brooke, D. Burns, E. Clement, D. Cussans, H. Flacher, J. Goldstein, M. Grimes, G.P. Heath, H.F. Heath, J. Jacob, L. Kreczko, C. Lucas, D.M. Newbold⁶⁴, S. Paramesvaran, A. Poll, T. Sakuma, S. Seif El Nasr-storey, D. Smith, V.J. Smith

Rutherford Appleton Laboratory, Didcot, United Kingdom

K.W. Bell, A. Belyaev⁶⁵, C. Brew, R.M. Brown, L. Calligaris, D. Cieri, D.J.A. Cockerill, J.A. Coughlan, K. Harder, S. Harper, E. Olaiya, D. Petyt, C.H. Shepherd-Themistocleous, A. Thea, I.R. Tomalin, T. Williams

Imperial College, London, United Kingdom

M. Baber, R. Bainbridge, O. Buchmuller, A. Bundock, D. Burton, S. Casasso, M. Citron, D. Colling, L. Corpe, P. Dauncey, G. Davies, A. De Wit, M. Della Negra, R. Di Maria, P. Dunne,

A. Elwood, D. Futyan, Y. Haddad, G. Hall, G. Iles, T. James, R. Lane, C. Laner, R. Lucas⁶⁴, L. Lyons, A.-M. Magnan, S. Malik, L. Mastrolorenzo, J. Nash, A. Nikitenko⁵⁰, J. Pela, B. Penning, M. Pesaresi, D.M. Raymond, A. Richards, A. Rose, C. Seez, S. Summers, A. Tapper, K. Uchida, M. Vazquez Acosta⁶⁶, T. Virdee¹⁶, J. Wright, S.C. Zenz

Brunel University, Uxbridge, United Kingdom

J.E. Cole, P.R. Hobson, A. Khan, P. Kyberd, D. Leslie, I.D. Reid, P. Symonds, L. Teodorescu, M. Turner

Baylor University, Waco, USA

A. Borzou, K. Call, J. Dittmann, K. Hatakeyama, H. Liu, N. Pastika

The University of Alabama, Tuscaloosa, USA

O. Charaf, S.I. Cooper, C. Henderson, P. Rumerio, C. West

Boston University, Boston, USA

D. Arcaro, A. Avetisyan, T. Bose, D. Gastler, D. Rankin, C. Richardson, J. Rohlf, L. Sulak, D. Zou

Brown University, Providence, USA

G. Benelli, E. Berry, D. Cutts, A. Garabedian, J. Hakala, U. Heintz, J.M. Hogan, O. Jesus, K.H.M. Kwok, E. Laird, G. Landsberg, Z. Mao, M. Narain, S. Piperov, S. Sagir, E. Spencer, R. Syarif

University of California, Davis, Davis, USA

R. Breedon, G. Breto, D. Burns, M. Calderon De La Barca Sanchez, S. Chauhan, M. Chertok, J. Conway, R. Conway, P.T. Cox, R. Erbacher, C. Flores, G. Funk, M. Gardner, W. Ko, R. Lander, C. Mclean, M. Mulhearn, D. Pellett, J. Pilot, S. Shalhout, J. Smith, M. Squires, D. Stolp, M. Tripathi, S. Wilbur, R. Yohay

University of California, Los Angeles, USA

C. Bravo, R. Cousins, A. Dasgupta, P. Everaerts, A. Florent, J. Hauser, M. Ignatenko, N. Mccoll, D. Saltzberg, C. Schnaible, E. Takasugi, V. Valuev, M. Weber

University of California, Riverside, Riverside, USA

K. Burt, R. Clare, J. Ellison, J.W. Gary, S.M.A. Ghiasi Shirazi, G. Hanson, J. Heilman, P. Jandir, E. Kennedy, F. Lacroix, O.R. Long, M. Olmedo Negrete, M.I. Paneva, A. Shrinivas, W. Si, H. Wei, S. Wimpenny, B. R. Yates

University of California, San Diego, La Jolla, USA

J.G. Branson, G.B. Cerati, S. Cittolin, M. Derdzinski, R. Gerosa, A. Holzner, D. Klein, V. Krutelyov, J. Letts, I. Macneill, D. Olivito, S. Padhi, M. Pieri, M. Sani, V. Sharma, S. Simon, M. Tadel, A. Vartak, S. Wasserbaech⁶⁷, C. Welke, J. Wood, F. Würthwein, A. Yagil, G. Zevi Della Porta

University of California, Santa Barbara - Department of Physics, Santa Barbara, USA

N. Amin, R. Bhandari, J. Bradmiller-Feld, C. Campagnari, A. Dishaw, V. Dutta, K. Flowers, M. Franco Sevilla, P. Geffert, C. George, F. Golf, L. Gouskos, J. Gran, R. Heller, J. Incandela, S.D. Mullin, A. Ovcharova, H. Qu, J. Richman, D. Stuart, I. Suarez, J. Yoo

California Institute of Technology, Pasadena, USA

D. Anderson, A. Apresyan, J. Bendavid, A. Bornheim, J. Bunn, Y. Chen, J. Duarte, J.M. Lawhorn, A. Mott, H.B. Newman, C. Pena, M. Spiropulu, J.R. Vlimant, S. Xie, R.Y. Zhu

Carnegie Mellon University, Pittsburgh, USA

M.B. Andrews, V. Azzolini, T. Ferguson, M. Paulini, J. Russ, M. Sun, H. Vogel, I. Vorobiev, M. Weinberg

University of Colorado Boulder, Boulder, USA

J.P. Cumalat, W.T. Ford, F. Jensen, A. Johnson, M. Krohn, T. Mulholland, K. Stenson, S.R. Wagner

Cornell University, Ithaca, USA

J. Alexander, J. Chaves, J. Chu, S. Dittmer, K. Mcdermott, N. Mirman, G. Nicolas Kaufman, J.R. Patterson, A. Rinkevicius, A. Ryd, L. Skinnari, L. Soffi, S.M. Tan, Z. Tao, J. Thom, J. Tucker, P. Wittich, M. Zientek

Fairfield University, Fairfield, USA

D. Winn

Fermi National Accelerator Laboratory, Batavia, USA

S. Abdullin, M. Albrow, G. Apollinari, S. Banerjee, L.A.T. Bauerdick, A. Beretvas, J. Berryhill, P.C. Bhat, G. Bolla, K. Burkett, J.N. Butler, H.W.K. Cheung, F. Chlebana, S. Cihangir[†], M. Cremonesi, V.D. Elvira, I. Fisk, J. Freeman, E. Gottschalk, L. Gray, D. Green, S. Grünendahl, O. Gutsche, D. Hare, R.M. Harris, S. Hasegawa, J. Hirschauer, Z. Hu, B. Jayatilaka, S. Jindariani, M. Johnson, U. Joshi, B. Klima, B. Kreis, S. Lammel, J. Linacre, D. Lincoln, R. Lipton, M. Liu, T. Liu, R. Lopes De Sá, J. Lykken, K. Maeshima, N. Magini, J.M. Marraffino, S. Maruyama, D. Mason, P. McBride, P. Merkel, S. Mrenna, S. Nahn, C. Newman-Holmes[†], V. O'Dell, K. Pedro, O. Prokofyev, G. Rakness, L. Ristori, E. Sexton-Kennedy, A. Soha, W.J. Spalding, L. Spiegel, S. Stoynev, J. Strait, N. Strobbe, L. Taylor, S. Tkaczyk, N.V. Tran, L. Uplegger, E.W. Vaandering, C. Vernieri, M. Verzocchi, R. Vidal, M. Wang, H.A. Weber, A. Whitbeck, Y. Wu

University of Florida, Gainesville, USA

D. Acosta, P. Avery, P. Bortignon, D. Bourilkov, A. Brinkerhoff, A. Carnes, M. Carver, D. Curry, S. Das, R.D. Field, I.K. Furic, J. Konigsberg, A. Korytov, J.F. Low, P. Ma, K. Matchev, H. Mei, G. Mitselmakher, D. Rank, L. Shchutska, D. Sperka, L. Thomas, J. Wang, S. Wang, J. Yelton

Florida International University, Miami, USA

S. Linn, P. Markowitz, G. Martinez, J.L. Rodriguez

Florida State University, Tallahassee, USA

A. Ackert, J.R. Adams, T. Adams, A. Askew, S. Bein, B. Diamond, S. Hagopian, V. Hagopian, K.F. Johnson, A. Khatiwada, H. Prosper, A. Santra

Florida Institute of Technology, Melbourne, USA

M.M. Baarmand, V. Bhopatkar, S. Colafranceschi, M. Hohlmann, D. Noonan, T. Roy, F. Yumiceva

University of Illinois at Chicago (UIC), Chicago, USA

M.R. Adams, L. Apanasevich, D. Berry, R.R. Betts, I. Bucinskaite, R. Cavanaugh, O. Evdokimov, L. Gauthier, C.E. Gerber, D.J. Hofman, K. Jung, P. Kurt, C. O'Brien, I.D. Sandoval Gonzalez, P. Turner, N. Varelas, H. Wang, Z. Wu, M. Zakaria, J. Zhang

The University of Iowa, Iowa City, USA

B. Bilki⁶⁸, W. Clarida, K. Dilsiz, S. Durgut, R.P. Gandrajula, M. Haytmyradov, V. Khristenko, J.-P. Merlo, H. Mermerkaya⁶⁹, A. Mestvirishvili, A. Moeller, J. Nachtman, H. Ogul, Y. Onel, F. Ozok⁷⁰, A. Penzo, C. Snyder, E. Tiras, J. Wetzel, K. Yi

Johns Hopkins University, Baltimore, USA

I. Anderson, B. Blumenfeld, A. Cocoros, N. Eminizer, D. Fehling, L. Feng, A.V. Gritsan, P. Maksimovic, C. Martin, M. Osherson, J. Roskes, U. Sarica, M. Swartz, M. Xiao, Y. Xin, C. You

The University of Kansas, Lawrence, USA

A. Al-bataineh, P. Baringer, A. Bean, S. Boren, J. Bowen, C. Bruner, J. Castle, L. Forthomme, R.P. Kenny III, S. Khalil, A. Kropivnitskaya, D. Majumder, W. Mcbrayer, M. Murray, S. Sanders, R. Stringer, J.D. Tapia Takaki, Q. Wang

Kansas State University, Manhattan, USA

A. Ivanov, K. Kaadze, Y. Maravin, A. Mohammadi, L.K. Saini, N. Skhirtladze, S. Toda

Lawrence Livermore National Laboratory, Livermore, USA

F. Rebassoo, D. Wright

University of Maryland, College Park, USA

C. Anelli, A. Baden, O. Baron, A. Belloni, B. Calvert, S.C. Eno, C. Ferraioli, J.A. Gomez, N.J. Hadley, S. Jabeen, R.G. Kellogg, T. Kolberg, J. Kunkle, Y. Lu, A.C. Mignerey, F. Ricci-Tam, Y.H. Shin, A. Skuja, M.B. Tonjes, S.C. Tonwar

Massachusetts Institute of Technology, Cambridge, USA

D. Abercrombie, B. Allen, A. Apyan, R. Barbieri, A. Baty, R. Bi, K. Bierwagen, S. Brandt, W. Busza, I.A. Cali, Z. Demiragli, L. Di Matteo, G. Gomez Ceballos, M. Goncharov, D. Hsu, Y. Iiyama, G.M. Innocenti, M. Klute, D. Kovalskyi, K. Krajczar, Y.S. Lai, Y.-J. Lee, A. Levin, P.D. Luckey, B. Maier, A.C. Marini, C. McGinn, C. Mironov, S. Narayanan, X. Niu, C. Paus, C. Roland, G. Roland, J. Salfeld-Nebgen, G.S.F. Stephans, K. Sumorok, K. Tatar, M. Varma, D. Velicanu, J. Veverka, J. Wang, T.W. Wang, B. Wyslouch, M. Yang, V. Zhukova

University of Minnesota, Minneapolis, USA

A.C. Benvenuti, R.M. Chatterjee, A. Evans, A. Finkel, A. Gude, P. Hansen, S. Kalafut, S.C. Kao, Y. Kubota, Z. Lesko, J. Mans, S. Nourbakhsh, N. Ruckstuhl, R. Rusack, N. Tambe, J. Turkewitz

University of Mississippi, Oxford, USA

J.G. Acosta, S. Oliveros

University of Nebraska-Lincoln, Lincoln, USA

E. Avdeeva, R. Bartek⁷¹, K. Bloom, D.R. Claes, A. Dominguez⁷¹, C. Fangmeier, R. Gonzalez Suarez, R. Kamalieddin, I. Kravchenko, A. Malta Rodrigues, F. Meier, J. Monroy, J.E. Siado, G.R. Snow, B. Stieger

State University of New York at Buffalo, Buffalo, USA

M. Alyari, J. Dolen, J. George, A. Godshalk, C. Harrington, I. Iashvili, J. Kaisen, A. Kharchilava, A. Kumar, A. Parker, S. Rappoccio, B. Roozbahani

Northeastern University, Boston, USA

G. Alverson, E. Barberis, A. Hortiangtham, A. Massironi, D.M. Morse, D. Nash, T. Orimoto, R. Teixeira De Lima, D. Trocino, R.-J. Wang, D. Wood

Northwestern University, Evanston, USA

S. Bhattacharya, K.A. Hahn, A. Kubik, A. Kumar, N. Mucia, N. Odell, B. Pollack, M.H. Schmitt, K. Sung, M. Trovato, M. Velasco

University of Notre Dame, Notre Dame, USA

N. Dev, M. Hildreth, K. Hurtado Anampa, C. Jessop, D.J. Karmgard, N. Kellams, K. Lannon,

N. Marinelli, F. Meng, C. Mueller, Y. Musienko³⁷, M. Planer, A. Reinsvold, R. Ruchti, G. Smith, S. Taroni, M. Wayne, M. Wolf, A. Woodard

The Ohio State University, Columbus, USA

J. Alimena, L. Antonelli, J. Brinson, B. Bylsma, L.S. Durkin, S. Flowers, B. Francis, A. Hart, C. Hill, R. Hughes, W. Ji, B. Liu, W. Luo, D. Puigh, B.L. Winer, H.W. Wulsin

Princeton University, Princeton, USA

S. Cooperstein, O. Driga, P. Elmer, J. Hardenbrook, P. Hebda, D. Lange, J. Luo, D. Marlow, J. Mc Donald, T. Medvedeva, K. Mei, M. Mooney, J. Olsen, C. Palmer, P. Piroué, D. Stickland, A. Svyatkovskiy, C. Tully, A. Zuranski

University of Puerto Rico, Mayaguez, USA

S. Malik

Purdue University, West Lafayette, USA

A. Barker, V.E. Barnes, S. Folgueras, L. Gutay, M.K. Jha, M. Jones, A.W. Jung, D.H. Miller, N. Neumeister, J.F. Schulte, X. Shi, J. Sun, F. Wang, W. Xie, L. Xu

Purdue University Calumet, Hammond, USA

N. Parashar, J. Stupak

Rice University, Houston, USA

A. Adair, B. Akgun, Z. Chen, K.M. Ecklund, F.J.M. Geurts, M. Guilbaud, W. Li, B. Michlin, M. Northup, B.P. Padley, R. Redjimi, J. Roberts, J. Rorie, Z. Tu, J. Zabel

University of Rochester, Rochester, USA

B. Betchart, A. Bodek, P. de Barbaro, R. Demina, Y.t. Duh, T. Ferbel, M. Galanti, A. Garcia-Bellido, J. Han, O. Hindrichs, A. Khukhunaishvili, K.H. Lo, P. Tan, M. Verzetti

Rutgers, The State University of New Jersey, Piscataway, USA

A. Agapitos, J.P. Chou, E. Contreras-Campana, Y. Gershtein, T.A. Gómez Espinosa, E. Halkiadakis, M. Heindl, D. Hidas, E. Hughes, S. Kaplan, R. Kunnawalkam Elayavalli, S. Kyriacou, A. Lath, K. Nash, H. Saka, S. Salur, S. Schnetzer, D. Sheffield, S. Somalwar, R. Stone, S. Thomas, P. Thomassen, M. Walker

University of Tennessee, Knoxville, USA

A.G. Delannoy, M. Foerster, J. Heideman, G. Riley, K. Rose, S. Spanier, K. Thapa

Texas A&M University, College Station, USA

O. Bouhali⁷², A. Celik, M. Dalchenko, M. De Mattia, A. Delgado, S. Dildick, R. Eusebi, J. Gilmore, T. Huang, E. Juska, T. Kamon⁷³, R. Mueller, Y. Pakhotin, R. Patel, A. Perloff, L. Perniè, D. Rathjens, A. Rose, A. Safonov, A. Tatarinov, K.A. Ulmer

Texas Tech University, Lubbock, USA

N. Akchurin, C. Cowden, J. Damgov, F. De Guio, C. Dragoiu, P.R. Duderod, J. Faulkner, E. Gурpinar, S. Kunori, K. Lamichhane, S.W. Lee, T. Libeiro, T. Peltola, S. Undleeb, I. Volobouev, Z. Wang

Vanderbilt University, Nashville, USA

S. Greene, A. Gurrola, R. Janjam, W. Johns, C. Maguire, A. Melo, H. Ni, P. Sheldon, S. Tuo, J. Velkovska, Q. Xu

University of Virginia, Charlottesville, USA

M.W. Arenton, P. Barria, B. Cox, J. Goodell, R. Hirosky, A. Ledovskoy, H. Li, C. Neu, T. Sinthuprasith, X. Sun, Y. Wang, E. Wolfe, F. Xia

Wayne State University, Detroit, USA

C. Clarke, R. Harr, P.E. Karchin, J. Sturdy

University of Wisconsin - Madison, Madison, WI, USA

D.A. Belknap, C. Caillol, S. Dasu, L. Dodd, S. Duric, B. Gomber, M. Grothe, M. Herndon, A. Hervé, P. Klabbers, A. Lanaro, A. Levine, K. Long, R. Loveless, I. Ojalvo, T. Perry, G.A. Pierro, G. Polese, T. Ruggles, A. Savin, N. Smith, W.H. Smith, D. Taylor, N. Woods

†: Deceased

1: Also at Vienna University of Technology, Vienna, Austria

2: Also at State Key Laboratory of Nuclear Physics and Technology, Peking University, Beijing, China

3: Also at Institut Pluridisciplinaire Hubert Curien, Université de Strasbourg, Université de Haute Alsace Mulhouse, CNRS/IN2P3, Strasbourg, France

4: Also at Universidade Estadual de Campinas, Campinas, Brazil

5: Also at Universidade Federal de Pelotas, Pelotas, Brazil

6: Also at Université Libre de Bruxelles, Bruxelles, Belgium

7: Also at Deutsches Elektronen-Synchrotron, Hamburg, Germany

8: Also at Joint Institute for Nuclear Research, Dubna, Russia

9: Also at Suez University, Suez, Egypt

10: Now at British University in Egypt, Cairo, Egypt

11: Also at Ain Shams University, Cairo, Egypt

12: Now at Helwan University, Cairo, Egypt

13: Also at Université de Haute Alsace, Mulhouse, France

14: Also at Skobeltsyn Institute of Nuclear Physics, Lomonosov Moscow State University, Moscow, Russia

15: Also at Tbilisi State University, Tbilisi, Georgia

16: Also at CERN, European Organization for Nuclear Research, Geneva, Switzerland

17: Also at RWTH Aachen University, III. Physikalisches Institut A, Aachen, Germany

18: Also at University of Hamburg, Hamburg, Germany

19: Also at Brandenburg University of Technology, Cottbus, Germany

20: Also at Institute of Nuclear Research ATOMKI, Debrecen, Hungary

21: Also at MTA-ELTE Lendület CMS Particle and Nuclear Physics Group, Eötvös Loránd University, Budapest, Hungary

22: Also at Institute of Physics, University of Debrecen, Debrecen, Hungary

23: Also at Indian Institute of Science Education and Research, Bhopal, India

24: Also at Institute of Physics, Bhubaneswar, India

25: Also at University of Visva-Bharati, Santiniketan, India

26: Also at University of Ruhuna, Matara, Sri Lanka

27: Also at Isfahan University of Technology, Isfahan, Iran

28: Also at University of Tehran, Department of Engineering Science, Tehran, Iran

29: Also at Yazd University, Yazd, Iran

30: Also at Plasma Physics Research Center, Science and Research Branch, Islamic Azad University, Tehran, Iran

31: Also at Università degli Studi di Siena, Siena, Italy

32: Also at Purdue University, West Lafayette, USA

33: Also at International Islamic University of Malaysia, Kuala Lumpur, Malaysia

34: Also at Malaysian Nuclear Agency, MOSTI, Kajang, Malaysia

35: Also at Consejo Nacional de Ciencia y Tecnología, Mexico city, Mexico

36: Also at Warsaw University of Technology, Institute of Electronic Systems, Warsaw, Poland

- 37: Also at Institute for Nuclear Research, Moscow, Russia
- 38: Now at National Research Nuclear University 'Moscow Engineering Physics Institute' (MEPhI), Moscow, Russia
- 39: Also at St. Petersburg State Polytechnical University, St. Petersburg, Russia
- 40: Also at University of Florida, Gainesville, USA
- 41: Also at P.N. Lebedev Physical Institute, Moscow, Russia
- 42: Also at California Institute of Technology, Pasadena, USA
- 43: Also at Budker Institute of Nuclear Physics, Novosibirsk, Russia
- 44: Also at Faculty of Physics, University of Belgrade, Belgrade, Serbia
- 45: Also at INFN Sezione di Roma; Università di Roma, Roma, Italy
- 46: Also at University of Belgrade, Faculty of Physics and Vinca Institute of Nuclear Sciences, Belgrade, Serbia
- 47: Also at Scuola Normale e Sezione dell'INFN, Pisa, Italy
- 48: Also at National and Kapodistrian University of Athens, Athens, Greece
- 49: Also at Riga Technical University, Riga, Latvia
- 50: Also at Institute for Theoretical and Experimental Physics, Moscow, Russia
- 51: Also at Albert Einstein Center for Fundamental Physics, Bern, Switzerland
- 52: Also at Gaziosmanpasa University, Tokat, Turkey
- 53: Also at Mersin University, Mersin, Turkey
- 54: Also at Cag University, Mersin, Turkey
- 55: Also at Piri Reis University, Istanbul, Turkey
- 56: Also at Adiyaman University, Adiyaman, Turkey
- 57: Also at Ozyegin University, Istanbul, Turkey
- 58: Also at Izmir Institute of Technology, Izmir, Turkey
- 59: Also at Marmara University, Istanbul, Turkey
- 60: Also at Kafkas University, Kars, Turkey
- 61: Also at Istanbul Bilgi University, Istanbul, Turkey
- 62: Also at Yildiz Technical University, Istanbul, Turkey
- 63: Also at Hacettepe University, Ankara, Turkey
- 64: Also at Rutherford Appleton Laboratory, Didcot, United Kingdom
- 65: Also at School of Physics and Astronomy, University of Southampton, Southampton, United Kingdom
- 66: Also at Instituto de Astrofísica de Canarias, La Laguna, Spain
- 67: Also at Utah Valley University, Orem, USA
- 68: Also at Argonne National Laboratory, Argonne, USA
- 69: Also at Erzincan University, Erzincan, Turkey
- 70: Also at Mimar Sinan University, Istanbul, Istanbul, Turkey
- 71: Now at The Catholic University of America, Washington, USA
- 72: Also at Texas A&M University at Qatar, Doha, Qatar
- 73: Also at Kyungpook National University, Daegu, Korea